

**NASA Contractor Report 181974**

**CORRELATION OF AH-1G AIRFRAME FLIGHT VIBRATION  
DATA WITH A COUPLED ROTOR-FUSELAGE ANALYSIS**

**K. Sangha and J. Shamie**

**McDonnell Douglas Helicopter Company  
Mesa, Arizona**

**Contract NAS1-17498  
August 1990**



National Aeronautics and  
Space Administration

**Langley Research Center**  
Hampton, Virginia 23665-5225

(NASA-CR-181974) CORRELATION OF AH-1G  
AIRFRAME FLIGHT VIBRATION DATA WITH A  
COUPLED ROTOR-FUSELAGE ANALYSIS  
(McDonnell-Douglas Helicopter Co.) 172 p

N90-28865

CSCL 20L 63/39 0303424  
Unclass



## FOREWORD

McDonnell Douglas Helicopter Company (MDHC) has been conducting a study of finite element modeling of helicopter airframes to predict vibration. This work is being performed under U.S. Government Contract NAS1-17498. The contract is monitored by the NASA Langley Research Center, Structures Directorate.

This report summarizes the procedure used at MDHC for predicting coupled rotor/fuselage vibrations with an application to the AH-1G two-bladed rotorcraft including comparisons with flight test vibrations. Key NASA and MDHC personnel are listed below.

### NASA Langley

Janice H. Clark, Contracting Officer

Joseph W. Owens, Contract Specialist

John H. Cline, Technical Representative

Raymond G. Kvaternik, Leader  
Rotorcraft Structural Dynamics Group

### McDonnell Douglas Helicopter Company

M. Toossi, Project Manager

R. King, Program Manager

K. Sangha, Rotor Dynamics

\*J. Shamie, Rotor Dynamics

\*Now with Hughes Aircraft Co.



# TABLE OF CONTENTS

<u>Section</u>	<u>Page</u>
Foreword	i
1. Introduction	1
2. Philosophy of Analytical Approach	5
3. Overall Capabilities of RACAP	9
4. Approach	13
4.1 Highlights of RACAP Formulation	15
4.2 RACAP Load Prediction Flow Chart	19
5. Airloads Model	23
5.1 Trim Analysis	25
5.2 Air Mass Dynamic Induced Inflow Modelling	31
5.2.1 Uniform Induced Inflow Model	35
5.2.2 Simple Nonuniform Induced Inflow Model	39
5.2.3 Wake Induced Inflow Model	43
5.2.4 Schematic of Wake Model	47
5.3 General Features of the Aerodynamics Model	51
5.4 Unsteady Aerodynamics Model	55
6. Blade Structural Model	59
6.1 Definition of Global (Hub-Fixed) Coordinate System	61
6.2 Global-Local Coordinate Transformation	69
6.3 Blade Element Representation	73
6.3.1 Flapwise Equilibrium and Compatibility	77
6.3.2 Chordwise Equilibrium and Compatibility	81
6.3.3 Torsion Equilibrium and Compatibility	85

## TABLE OF CONTENTS (continued)

<u>Section</u>	<u>Page</u>
6.4 Blade Cross Section Definition	89
6.5 Spanwise Distribution of Structural, Inertial, and Geometric Properties	93
7. Blade Root End Modeling Capabilities	97
7.1 Articulated Rotors	99
7.2 Teetering Rotors	103
7.3 Hingeless/Bearingless Rotors	107
8. Blade Forced Response Transfer Matrix Solution Technique	111
8.1 Blade Element Transfer Matrix Model	113
8.2 Blade Transfer Matrix Relations	117
9. Coupled Rotor/Airframe Forces Response Formulation	127
9.1 Overall Approach	129
9.2 Solution Technique	133
9.2.1 Rotor Impedance Formulation	135
9.2.2 Airframe Impedance Calculation	139
9.2.3 Relationship of Rotating and Fixed System Displacements and Forces	143
9.2.4 Inboard Hinge Moment Equilibrium Equations	147
9.2.5 Boundary Condition Formulation Using Harmonic Analysis Approach	151
9.3 Coupled Rotor/Airframe Forced Response	155
10. Analysis and Correlation Plan	161
10.1 AH-1G Blade Structural Modeling	165
10.2 AH-1G Aerodynamics Model	166

TABLE OF CONTENTS (continued)

<u>Section</u>	<u>Page</u>
10.3 AH-1G Airframe Model	173
10.4 Coupled Rotor-Fuselage Analysis	177
11. Discussion of Results	181
11.1 Results	185
12. Concluding Remarks	211
13. References	215
14. Appendix	219

PRECEDING PAGE BLANK NOT FILMED

ORIGINAL PAGE IS  
OF POOR QUALITY





---

## **1.0 INTRODUCTION**

## INTRODUCTION

The need for developing and implementing improved capabilities for accurately determining rotor/airframe response loads is well recognized. Presently, reduction of rotor/airframe loads to an acceptable level in many cases required intensive, costly, time and payload consuming design modifications. The NASA Langley Research Center is sponsoring a rotorcraft structural dynamics program with the overall objective to establish in the United States a superior capability to utilize finite element analysis models for calculations to support industrial design of helicopter airframe structures. Viewed as a whole, the program is planned to include efforts by NASA, Universities, and the U.S. Helicopter Industry. In the initial phase of the program, teams from the major U.S. manufacturers of helicopter airframes will apply extant finite element analysis methods to calculate static internal loads and vibrations of helicopter airframes of both metal and composite construction, conduct laboratory measurements of the structural behavior of these airframe, and perform correlations between analysis and measurements to build up a basis upon which to evaluate the results of the applications. To maintain the necessary scientific observation and control, emphasis throughout these activities will be on advance planning, documentation of methods and procedures, an thorough discussion of results and experiences, all with industry-wide critique to allow maximum technology transfer between companies. The finite element models formed in this phase will then serve as the basis for the development, application and evaluation of both improved modeling techniques and advanced analytical and computational techniques, all aimed at strengthening and enhancing the technology base which supports industrial design of helicopter airframe structures. Here again, procedures for mutual critique have been established, and these procedures call for a thorough discussion among the program participants of each method prior to the applications and of the results and experiences after the applications.

This report is a description of an analysis method, plan and results obtained in calculating coupled rotor/ airframe flight vibration levels for a helicopter in steady state forward flight. The method used is MDHC's Rotor Airframe Comprehensive Aeroelastic Program (RACAP).

---

## **2.0 PHILOSOPHY OF ANALYTICAL APPROACH**

PRECEDING PAGE BLANK NOT FILMED

## **PHILOSOPHY OF ANALYTICAL APPROACH**

RACAP is a comprehensive rotorcraft design and analysis tool which has been formulated with state-of-the-art philosophy in helicopter aeroelasticity. In the structural representation of blade elements emphasis is placed on completeness of the model. Coupling of the rotor with the fuselage is performed in an accurate manner. The aerodynamic model has been developed with provision for updating airloads, unsteady aerodynamics, and inflow modelling. A modular approach is used for ease of interchangeability and improvement of analytical methods.

## **PHILOSOPHY OF ANALYTICAL APPROACH**

---

- **“COMPLETENESS” IN STRUCTURAL REPRESENTATION OF BLADE ELEMENTS**
- **PROVISION FOR ACCURATE COUPLING OF ROTOR WITH FUSELAGE**
- **AERODYNAMIC MODULE WITH PROVISION FOR UPDATE OF**
  - **AIRLOADS**
  - **UNSTEADY AERODYNAMICS**
  - **INFLOW MODEL**
- **MODULAR APPROACH FOR EASE OF INTERCHANGEABILITY AND UPGRADE OF ANALYTICAL METHODS**



---

### **3.0 OVERALL CAPABILITIES OF RACAP**

PRECEDING PAGE BLANK NOT FILMED

## OVERALL CAPABILITIES OF RACAP

RACAP serves as a comprehensive aeroelastic computational program for prediction of rotor/airframe characteristics. Included in the existing capabilities of RACAP are: 1) rotor aeroelastic loads prediction, 2) airload calculation for use in far-field noise prediction, 3) free vibration analysis, 4) fuselage vibration prediction, 6) calculation of performance characteristics, 7) prediction of performance and vibration effects of Higher Harmonic Control for all rotor and fuselage configurations and 8) bearingless rotor analyses including details of the multiple load paths.



## **OVERALL CAPABILITIES OF RACAP**

---

**A COUPLED ROTOR/AIRFRAME FINITE ELEMENT PROGRAM  
FOR:**

- **ROTOR AEROELASTIC LOADS PREDICTION**
- **AIRLOADS CALCULATION FOR USE IN FAR-FIELD NOISE PREDICTION**
- **FREE VIBRATION ANALYSIS**
- **FUSELAGE VIBRATION PREDICTION**
- **PERFORMANCE CHARACTERISTICS**
- **PERFORMANCE AND VIBRATION EFFECTS OF HIGHER HARMONIC CONTROL FOR ALL ROTOR (ARTICULATED, TEETERING, HINGELESS, AND BEARINGLESS) AND FUSELAGE CONFIGURATIONS**



---

## 4.0 APPROACH



---

## 4.1 HIGHLIGHTS OF RACAP FORMULATION

PRECEDING PAGE IMAGE NOT FILMED

## HIGHLIGHTS OF RACAP FORMULATION

The approach employed in RACAP performs rotor trim and airloads calculations in the time domain. The coupled rotor/airframe analysis is based on coupling a state-of-the-art aeroelastic rotor loads model formulated using the transfer matrix approach, with a NASTRAN finite element/experimental airframe model. Impedance matching at the hub performed with a 6 degree-of-freedom hub impedance matrix in combination with a harmonic balance solution is used in the coupling procedure. The structural response of the blades is obtained as a superposition of the harmonic responses due to harmonic loads. Fuselage vibrations are determined by subsequently applying the calculated hub loads to the NASTRAN finite element model.

## HIGHLIGHTS OF RACAP FORMULATION

---

**RACAP IS BASED ON:**

- ROTOR TRIM AND AIRLOAD CALCULATIONS PERFORMED IN THE TIME DOMAIN
- ROTOR TRANSFER MATRIX APPROACH
- FUSELAGE 6 D.O.F. HUB IMPEDANCE MATRIX AND AIRFRAME DYNAMICS OBTAINED USING A NASTRAN FINITE ELEMENT MODEL
- ROTOR/AIRFRAME COUPLING THROUGH IMPEDANCE MATCHING AT ROTOR HUB IN COMBINATION WITH A HARMONIC BALANCE SOLUTION
- BLADE STRUCTURAL RESPONSE OBTAINED AS SUPERPOSITION OF RESPONSES DUE TO HARMONIC LOADS
- HUB LOADS [SUBSEQUENTLY] USED TO CALCULATE FUSELAGE VIBRATION USING FINITE ELEMENT MODEL





---

## 4.2 RACAP LOAD PREDICTION FLOW CHART

PRECEDING PAGE BLANK NOT FILMED

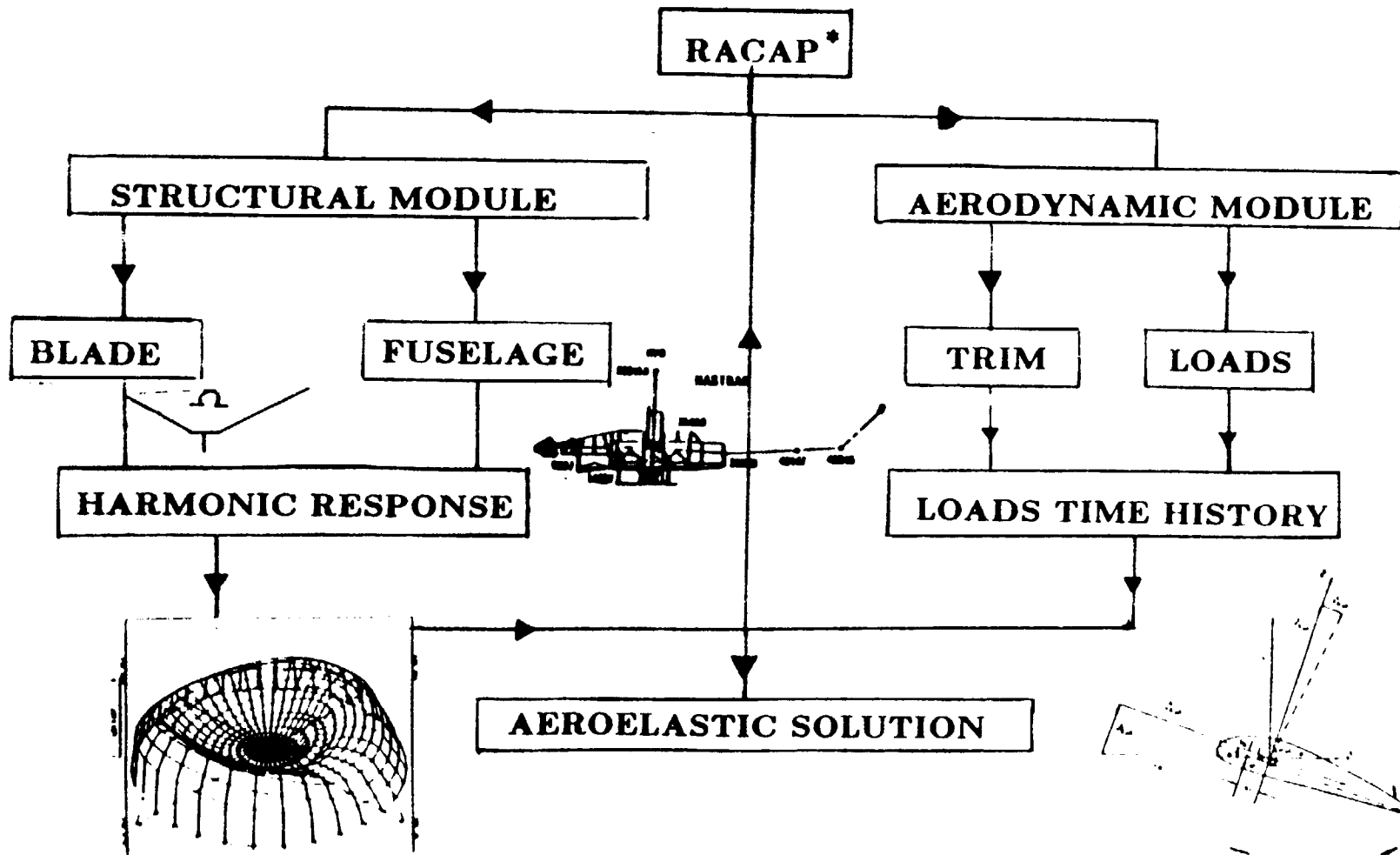
## RACAP LOADS PREDICTION FLOW CHART

The general helicopter aeroelastic problem is divided into six major categories:

1. Air mass dynamics (induced inflow modeling)
2. Calculation of aerodynamic loads
3. Rotor blade dynamics
4. Blade/fuselage coupling
5. Determination of control inputs
6. Fuselage dynamics

Coupled rotor/fuselage blade dynamic response is obtained in the frequency domain. The harmonics are combined into a time history of response that is used in the aerodynamics module to compute new estimates of control angles (trim) and aerodynamic loads. The new loads and control angles are used in the structural module. The process is repeated iteratively until a converged aeroelastic solution is obtained.

# ROTOR LOADS PREDICTION FLOWCHART



ORIGINAL PAGE IS  
OF POOR QUALITY

\* Rotor/Airframe Comprehensive Aeroelastic Program



---

## 5.0 AIRLOADS MODEL



---

## 5.1 TRIM ANALYSIS

PROCESSED FROM 1957 FILMED

## TRIM ANALYSIS

The purpose of the trim analysis is to provide control inputs (main rotor collective and cyclic pitches) and an initial estimate of the rotor airloads for use in RACAP. This is done initially using a rigid blade model, in an external program. An isolated rotor trim algorithm is typically used to trim the rotor for a given lift and propulsive force using two rotor control variables: the main rotor collective and longitudinal cyclic pitches. The trim program uses a lifting line model to evaluate the forces and moments acting on the rotor blade. Subsequent to the first aeroelastic iteration, the control settings are obtained as a function of the elastic deformation within RACAP, using a Newton-Raphson or Secant method approach. A longitudinal thrust and propulsive force trim only is performed.



## TRIM ANALYSIS

---

- PROVIDES CONTROL INPUTS AND INITIAL MAIN ROTOR AIRLOADS
- ISOLATED ROTOR: TRIM ON LIFT AND PROPULSIVE FORCES.  
USES 2 TRIM VARIABLES (MAIN ROTOR  
COLLECTIVE AND LONGITUDINAL CYCLIC  
PITCHES) TO TRIM
- FORCES AND MOMENTS DUE TO MAIN ROTOR EVALUATED USING  
LIFTING LINE MODEL FOR BLADE AERODYNAMICS

## TRIM ANALYSIS

The main rotor model consists of  $N$  blades equally spaced wherein each blade is identical to the other and is defined by one degree of freedom. The blade is restricted to rigid flapping motion, since the Tip-Path-Plane tilt is the primary contributor to trimmed control angles. Blade dynamic equations are solved in the time domain and the periodic blade motion is obtained using a numerical integration scheme. The model uses a lifting line (or blade element) theory along with measured 2D airfoil characteristics to compute airloads in the time domain and has the option to use either a simple nonuniform induced inflow (Glauert's) model or a free or rigid wake model to determine the induced velocity at the rotor disk. The effects of tip-loss and tip Mach relief are also included.

The basic trim procedure consists of comparing the current solution for the forces and moments on the helicopter (or rotor) with the target values and incrementing the control variables in a manner required to approach the targets in the next cycle. The increments in the control variables are obtained with the help of a numerically evaluated trim sensitivity matrix. Once the trimmed state along with a periodic blade motion solution is calculated, main rotor airloads are harmonically analyzed and are provided as initial values for use in RACAP.

## TRIM ANALYSIS (continued)

---

- **MAIN ROTOR MODEL:**
  - **ISOLATED ROTOR TRIM ANALYSIS USES BLADE FLAPPING DEGREE OF FREEDOM ONLY.**
  - **BLADE DYNAMIC EQUATIONS ARE SOLVED IN THE TIME DOMAIN USING NUMERICAL INTEGRATION SCHEME**
  - **LIFTING LINE (BLADE ELEMENT) THEORY ALONG WITH EXPERIMENTAL TWO-DIMENSIONAL AIRFOIL DATA ARE USED TO COMPUTE THE AIRLOADS IN THE TIME DOMAIN**
  - **OPTION TO USE EITHER SIMPLE NONUNIFORM (Glauert's) INFLOW MODEL OR RIGID OR FREE WAKE INDUCED INFLOW MODEL**
- **ONCE TRIM IS OBTAINED, AIRLOADS ARE HARMONICALLY ANALYZED AND ARE PROVIDED AS INITIAL VALUES TO RACAP**



---

## **5.2 AIR MASS DYNAMICS (INDUCED INFLOW MODELLING)**

## INDUCED INFLOW MODELLING

RACAP has provisions to use three different induced inflow models in its main rotor model. They are (i) uniform induced inflow, (ii) simple non-uniform induced inflow (Glauert's model) and (iii) rigid or free vortex wake induced inflow.

## **INDUCED INFLOW MODELING**

---

- **RACAP HAS PROVISION TO USE THREE DIFFERENT INDUCED INFLOW MODELS**
  - **UNIFORM INDUCED INFLOW**
  - **SIMPLE NON-UNIFORM INDUCED INFLOW (GLAUERT'S MODEL)**
  - **RIGID OR FREE WAKE INDUCED INFLOW**





---

### **5.2.1 UNIFORM INDUCED INFLOW MODEL**

PHOTOCOPIED FROM FILM NOT FILMED

## **UNIFORM INDUCED INFLOW MODEL**

The induced velocity over the main rotor disk is assumed to be constant and is evaluated using simple momentum theory.

## **UNIFORM INDUCED INFLOW MODEL**

---

- **UNIFORM INDUCED INFLOW MODEL**
  - **INDUCED VELOCITY OVER THE MAIN ROTOR DISK IS ASSUMED TO BE CONSTANT**
  - **INDUCED VELOCITY EVALUATED USING SIMPLE MOMENTUM THEORY**



---

### **5.2.2 SIMPLE NONUNIFORM INDUCED INFLOW MODEL**

## **SIMPLE NON-UNIFORM INDUCED INFLOW MODEL**

This model assumes a linear induced inflow variation in the fore and aft direction of the rotor disk (Glauert's model). This inflow variation results in a first harmonic variation in the induced velocity around the azimuth. This model incorporates the effect of net aerodynamic moments (pitching and rolling moments) on the rotor disk.

## **SIMPLE NON-UNIFORM INDUCED INFLOW MODEL**

---

- **INDUCED INFLOW IS ASSUMED TO VARY LINEARLY IN THE FORE AND AFT DIRECTION AROUND THE AZIMUTH**





---

### **5.2.3 WAKE INDUCED INFLOW MODEL**

PRECEDING PAGE SHOULD NOT BE FILMED

## VORTEX WAKE INDUCED INFLOW MODEL

This inflow model uses a deformed wake analysis program originally developed by the RASA Division of Systems Research Laboratories (Ref. 1). For a given set of flight conditions, this model generates a set of wake influence coefficients to iteratively generate non-uniform wake induced velocities over the main rotor disk. The wake program has the option of using either a free (deformed) or rigid (prescribed) wake geometry depending on the flight condition. Each blade is modeled as a lifting line, with a mesh of concentrated shed and trailed vorticity following each lifting line in the near wake. The far wake has only trailed vorticity. The generation of wake geometry is done by a process similar to start-up of a rotor in a free stream. In a general free-wake model, the wake elements are allowed to freely distort in the generation process. Vortex element end points (wake points) are allowed to be transported by the resultant of the free-stream and vortex-induced velocities. For high-speed flight conditions, a rigid wake geometry where the wake vortex elements are convected by the resultant of the free-stream velocity and an average induced velocity (determined from momentum considerations) is used.

## **VORTEX WAKE INDUCED INFLOW MODEL**

---

- **USES VORTEX WAKE MODEL ORIGINALLY DEVELOPED BY RASA**
  - **EACH BLADE IS MODELED AS A LIFTING LINE**
  - **MESH OF SHED AND TRAILED VORTEX ELEMENTS WITH RIGID FINITE CORES (FULL MESH) BEHIND EACH BLADE IN THE NEAR WAKE**
  - **TRAILING VORTEX ELEMENTS (MODIFIED MESH) ONLY IN THE FAR WAKE**
  - **WAKE GEOMETRY GENERATED BY A PROCESS SIMILAR TO START UP OF A ROTOR IN FREE STREAM**
- **OPTION OF USING EITHER A FREE (DEFORMED) OR RIGID (PRESCRIBED) WAKE GEOMETRY DEPENDING ON THE FLIGHT CONDITION**
- **GENERATION OF WAKE INFLUENCE COEFFICIENTS FOR ITERATIVELY DETERMINING NON-UNIFORM WAKE INDUCED VELOCITIES OVER THE MAIN ROTOR DISK**



---

#### **5.2.4 SCHEMATIC OF WAKE GEOMETRY ELEMENTS**

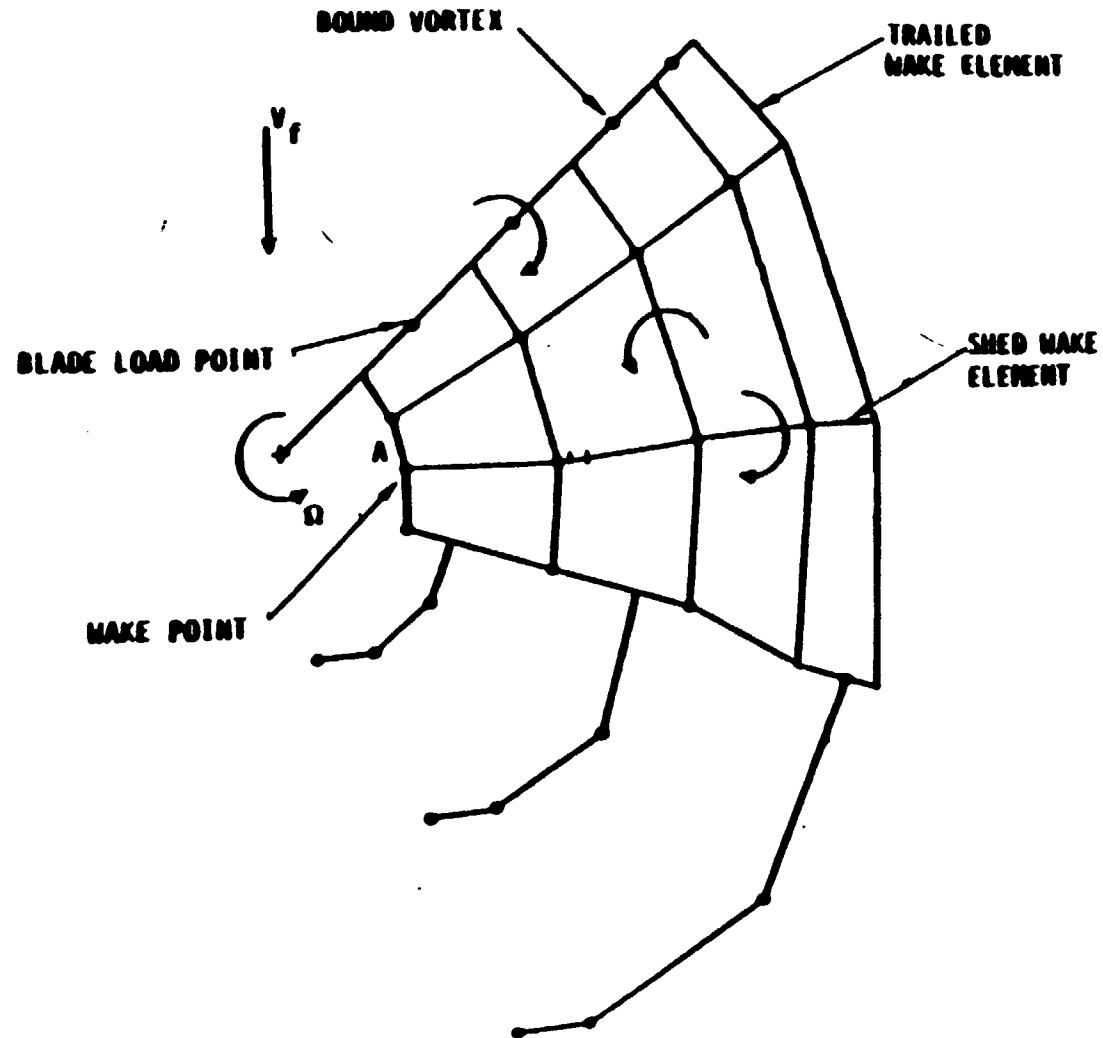
PRECEDING PAGE BLANK NOT FILMED

## WAKE GEOMETRY MODEL

The wake model, as shown in the figure, has a mesh of shed and trailed vortices immediately behind each blade (modeled as a lifting line bound vortex), followed by a set of one or more trailing vortices for the remainder of the wake. The vortex elements are straight with finite cores and have uniform strength and core radius along each vortex element length. Depending on the advance ratio, a chosen number of revolutions of the rotor is retained for determining the induced velocities at the rotor disk. The induced velocities at the wake points and the blade load points are evaluated using the Biot-Savart law.

## WAKE GEOMETRY MODEL

---



ORIGINAL PAGE IS  
OF POOR QUALITY





---

### **5.3 GENERAL FEATURES OF THE AERODYNAMICS MODEL**

PRECEDING PAGE BLANK NOT FILMED

## GENERAL FEATURES OF THE AERODYNAMICS MODEL

The aerodynamics model uses lifting line (or blade element) theory along with measured two-dimensional airfoil characteristics to calculate the blade section airloads. For conditions below stall, an unsteady aerodynamic model based on thin airfoil theory is used. Dynamic stall effects are evaluated using semi-empirical models. Simple formulations are used to consider the effects of radial flow on the blades, three dimensional effects near the blade tips and reverse flow. The airload computations are made in the time domain and include the effects of rigid and elastic deformations. The aerodynamics model has the option of using any one of the different induced inflow models described earlier. If the vortex wake induced inflow model is used, inflow iterations are made to get a compatible set of induced velocities and blade airloads. The airload computations are then iterated with the blade response solution to get a compatible set of blade airloads and deformations.

## **GENERAL FEATURES OF THE AERODYNAMICS MODEL**

---

- **LIFTING LINE (OR BLADE ELEMENT) THEORY IN COMBINATION WITH EXPERIMENTAL TWO-DIMENSIONAL AIRFOIL CHARACTERISTICS**
- **UNSTEADY AERODYNAMICS BASED ON THIN AIRFOIL THEORY**
- **SEMI-EMPIRICAL DYNAMIC STALL MODEL**
- **SIMPLE FORMULATIONS TO CONSIDER THE EFFECTS OF RADIAL FLOW ON THE BLADES, THREE DIMENSIONAL EFFECTS NEAR THE TIPS, AND REVERSE FLOW**
- **EFFECTS OF RIGID AND ELASTIC BLADE MOTIONS CONSIDERED**
- **AIRLOAD COMPUTATIONS MADE IN THE TIME DOMAIN**
- **FOR THE CASE OF VORTEX WAKE INDUCED INFLOW, INFLOW ITERATIONS PERFORMED TO OBTAIN A COMPATIBLE SET OF INDUCED VELOCITIES AND BLADE AIRLOADS**
- **AIRLOAD CALCULATIONS ITERATED WITH BLADE RESPONSE SOLUTION**



---

## **5.4 UNSTEADY AERODYNAMICS MODEL**

PRECEDING PAGE BLANK NOT FILMED

## UNSTEADY AERODYNAMICS

For conditions below stall, the effects of unsteady aerodynamics are included in the airloads computations using unsteady thin airfoil theory suitably modified for rotors. The effects of radial flow along the blades and the time varying onset flow and corrections for real flow effects on the lift curve slope and aerodynamic center are included in the expressions used for unsteady lift and pitching moment. No unsteady drag effects are included for conditions below stall. For dynamic stall conditions, provision is made to use the following semi-empirical model:

Time delay model: The effects of stall on lift and pitching moments are delayed to higher angles of attack using experimentally determined time delay constants. The effects of vortices shed from the leading edge are included (depending on the pitch rate) using an empirical model originally developed at Massachusetts Institute of Technology.

## UNSTEADY AERODYNAMICS

---

- **USE OF THIN AIRFOIL THEORY SUITABLY MODIFIED FOR ROTORS IN CONDITIONS BELOW STALL. EFFECTS OF RADIAL FLOW ALONG THE BLADES, TIME VARYING ONSET FLOW AND CORRECTIONS FOR REAL FLOW EFFECTS ON THE LIFT CURVE SLOPE AND AERODYNAMIC CENTER ARE INCLUDED IN THE EXPRESSIONS FOR LIFT AND PITCHING MOMENT**
- **NO UNSTEADY DRAG EFFECTS BELOW STALL**





---

## **6.0    BLADE STRUCTURAL MODEL**

PRECEDING PAGE BLANK NOT FILMED



---

## **6.1    DEFINITION OF GLOBAL COORDINATE SYSTEM DOFs**

PRECEDING PAGE BLANK NOT FILMED

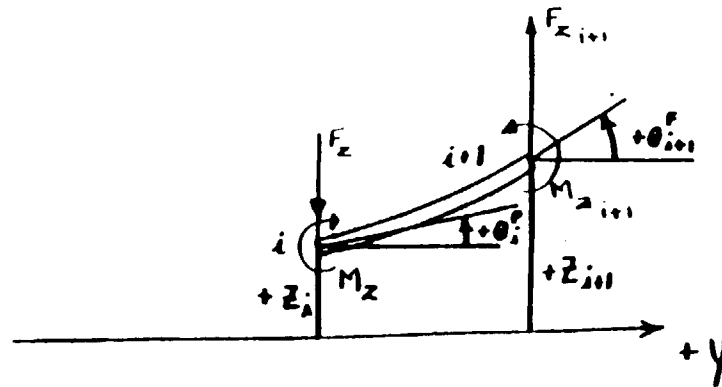
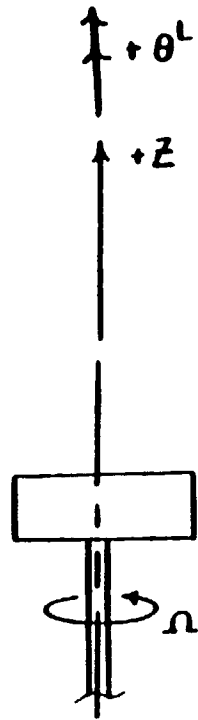
## DEFINITION OF GLOBAL (HUB FIXED) COORDINATE SYSTEM

A right hand coordinate system which is used for measuring global (hub fixed, rotating) or shaft axis deformations is established and variables which locate the deformed position at each station of the blade are defined. These are rotations and displacements in flap, lag and axial directions. The rotation about the axial direction is elastic/kinematic torsion, while the axial displacement is entirely kinematic. The global coordinate system is defined as -X aft, -Y outboard along the blade and -Z vertically upward. The constitutive equilibrium and compatibility equations are derived in a local right-handed system fixed at the shear center of the deformed blade, and then transformed to the global, hub-fixed system in the undeformed geometry.

# DEFINITION OF GLOBAL (HUB FIXED) COORDINATE SYSTEM

## FLAPWISE STATE VARIABLES

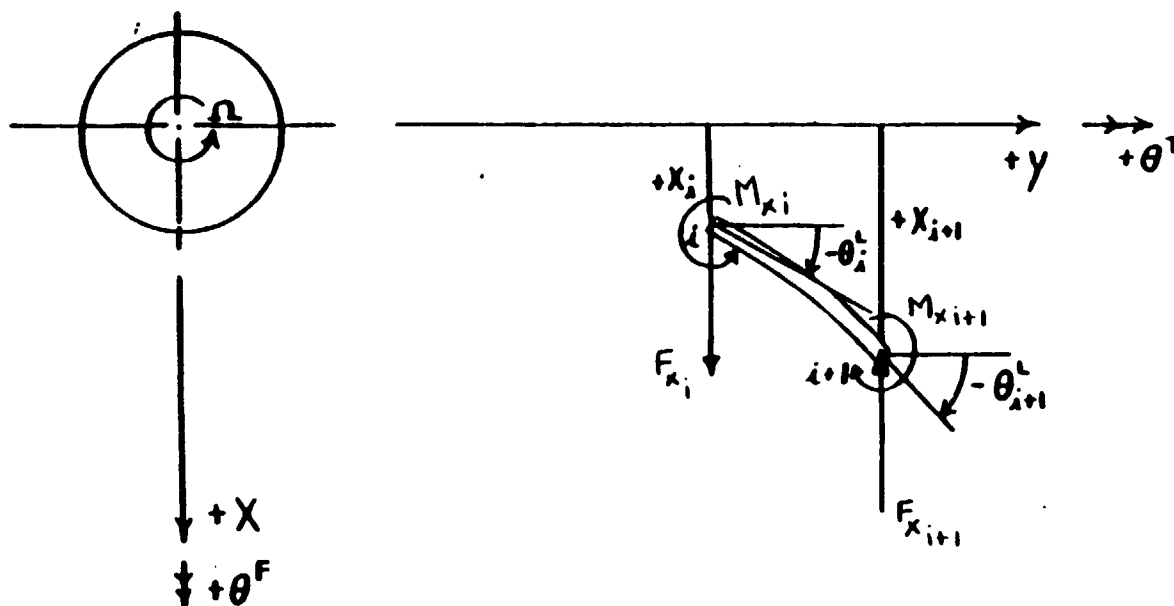
ORIGIN, FACE IS  
OF POOR QUALITY



## **Definition of Global Hub Coordinate System Lag DOFs**

# DEFINITION OF GLOBAL (HUB FIXED) COORDINATE SYSTEM (continued)

## CHORDWISE STATE VARIABLES



## **DEFINITION OF GLOBAL COORDINATE SYSTEM TORSION DOFs.**

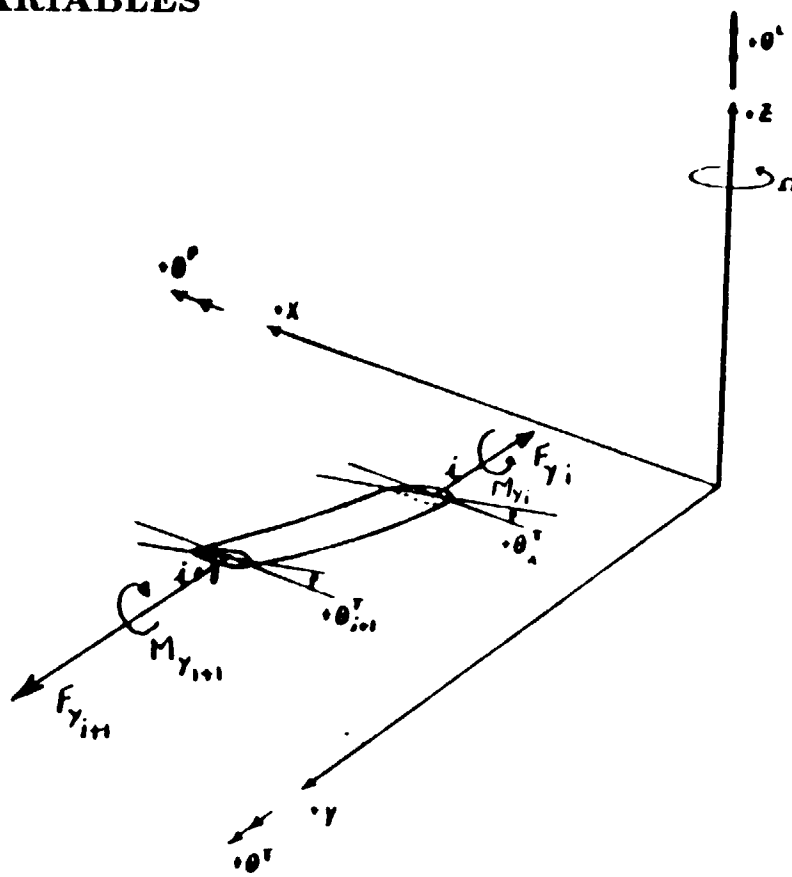


# DEFINITION OF GLOBAL COORDINATE SYSTEM

## TORSION DOFs (continued)

---

### TORSION STATE VARIABLES





---

## **6.2 GLOBAL-LOCAL COORDINATE TRANSFORMATION**

PRECEDING PAGE BLANK NOT FILMED

## GLOBAL-LOCAL COORDINATE TRANSFORMATION

A transformation from the global to local coordinates is defined. The transformation is completely general and no small angle assumptions are made. Rotations are treated as vectors and a sequence of rotations (Torsion, Lag, Flap) is adopted and adhered to in the entire derivation. The transformation employs rotations about the global (undeformed) coordinate system. The final, nonlinear transformation is between the local system rotated through flap-lag-torsion angles calculated for the station of interest, and the global, hub - fixed system. Both coordinate systems are orthogonal.

## GLOBAL-LOCAL COORDINATE TRANSFORMATION

---

### GLOBAL-LOCAL COORDINATE TRANSFORMATION AT STATION $i$

$$\begin{Bmatrix} \hat{e}_x \\ \hat{e}_y \\ \hat{e}_z \end{Bmatrix}_G = [ f(\theta_i^F, \theta_i^L, \theta_i^T) ] \begin{Bmatrix} \hat{e}_x \\ \hat{e}_y \\ \hat{e}_z \end{Bmatrix}_L$$

- LOCAL COORDINATE SYSTEM IS ATTACHED TO THE SHEAR CENTER OF THE DEFORMED BLADE CROSS SECTION AT STATION  $i$
- $\theta^T, \theta^L, \theta^F$  SEQUENCE OF ROTATIONS WITH RESPECT TO GLOBAL (HUB-FIXED) COORDINATE SYSTEM





## **6.3 BLADE ELEMENT REPRESENTATION**

PRECEDING PAGE BLANK NOT FILMED

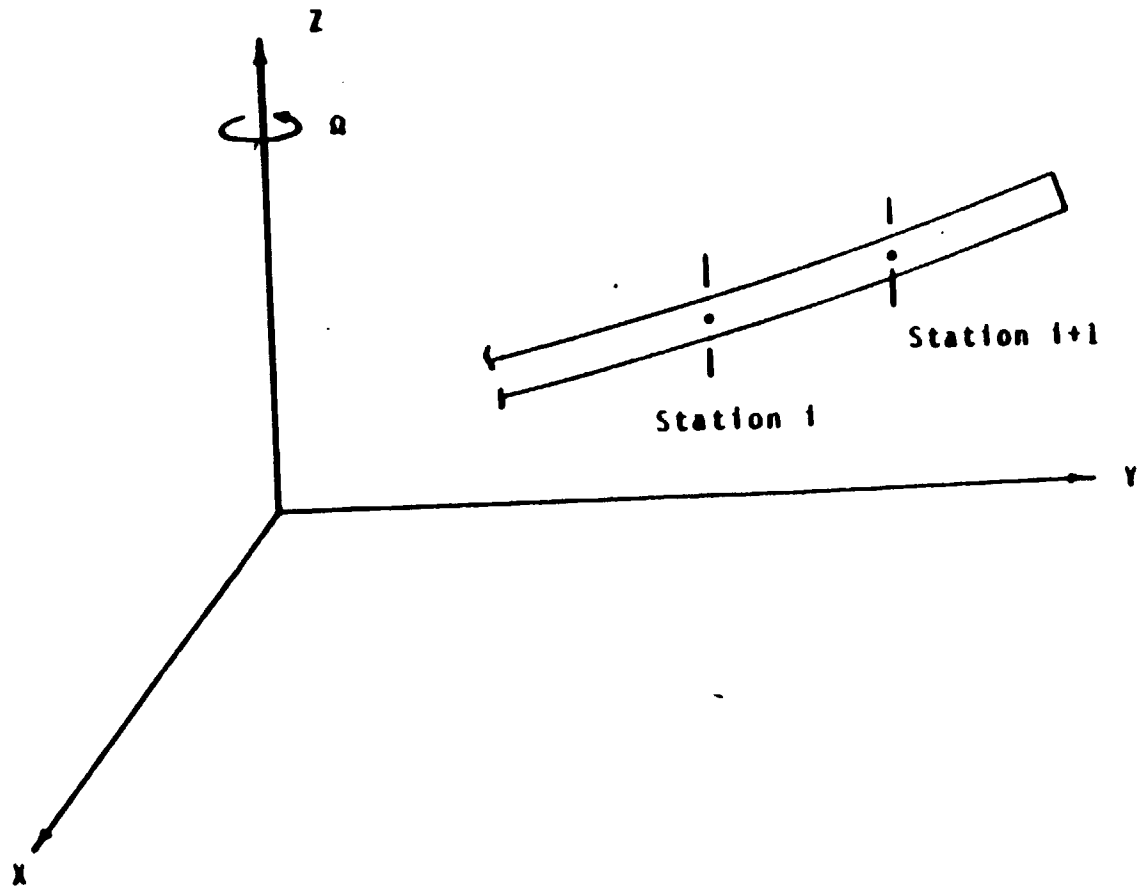
## **BLADE ELEMENT REPRESENTATION**

The transfer matrix method equations are obtained by considering force and moment equilibrium and displacement and rotation compatibility of a beam element located between stations  $i$  and  $i+1$ . All equations are formulated using state variables (moments, forces, displacements, and rotations) defined in the global coordinate system. The flapwise and chordwise bending moments are calculated with respect to the neutral axis whereas the torsional moments are calculated with respect to the shear center.



## BLADE ELEMENT REPRESENTATION

---





---

### **6.3.1 FLAPWISE EQUILIBRIUM AND COMPATABILITY**

PRECEDING PAGE BLANK NOT FILMED

## FLAPWISE EQUILIBRIUM AND COMPATIBILITY

---

### FLAPWISE MOTION:

FORCE EQUILIBRIUM:

MOMENT EQUILIBRIUM:

Z DISPLACEMENT:

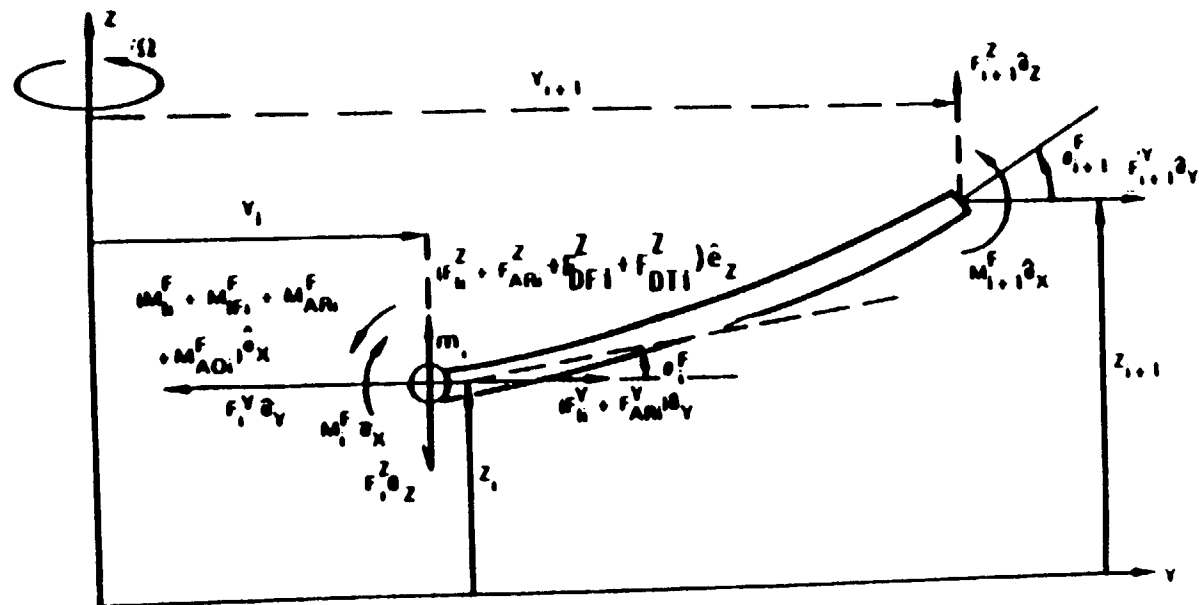
$\theta^F$  ROTATION:

$$\begin{aligned}
 F_i^Z &= F_I^Z + F_{i+1}^Z + F_{ARi}^Z + F_{DTi}^Z \\
 M_i^F &= M_{i+1}^F + F_{i+1}^Z (Y_{i+1} - Y_i) - F_{i+1}^Y (Z_{i+1} - Z_i) \\
 &\quad + M_{Ii}^F + M_{IFi}^F + M_{ARi}^F + M_{AOi}^F \\
 Z_i &= Z_{i+1} - \ell_{i,i+1} c \theta_i^L s \theta_i^F - Z_{i+1}^{elastic} - Z_{i+1}^{kinematic} \\
 \theta_i^F &= \theta_{i+1}^F - \theta_{i+1}^{elastic} - \theta_{i+1}^{built-in}
 \end{aligned}$$

WHERE FOR STATION  $i$

- $F_I^Z$  = INERTIA FORCE ,  $F_{AR}^Z$  = AERODYNAMIC FORCE
- $F_{DF}^Z$  = AERODYNAMIC DAMPING FORCE DUE TO MOTION IN THE Z-DIRECTION
- $F_{DT}^Z$  = AERODYNAMIC DAMPING FORCE DUE TO PITCHING MOTION
- $M_I^F$  = INERTIA MOMENT ABOUT THE X-AXIS
- $M_{IF}^F$  = MOMENT OF THE INERTIA FORCES ABOUT THE X-AXIS DUE TO CROSS SECTIONAL OFFSETS
- $M_{AR}^F$  = AERODYNAMIC MOMENT ABOUT THE X-AXIS
- $M_{AO}^F$  = MOMENT ABOUT THE X-AXIS OF THE AERODYNAMIC FORCES DUE TO SHEAR CENTER OFFSET FROM NEUTRAL-AXIS

# FLAPWISE EQUILIBRIUM AND COMPATIBILITY





---

### **6.3.2 CHORDWISE EQUILIBRIUM AND COMPATIBILITY**

PRECEDING PAGE BLANK NOT FILMED

## CHORDWISE EQUILIBRIUM AND COMPATIBILITY

---

### CHORDWISE MOTION:

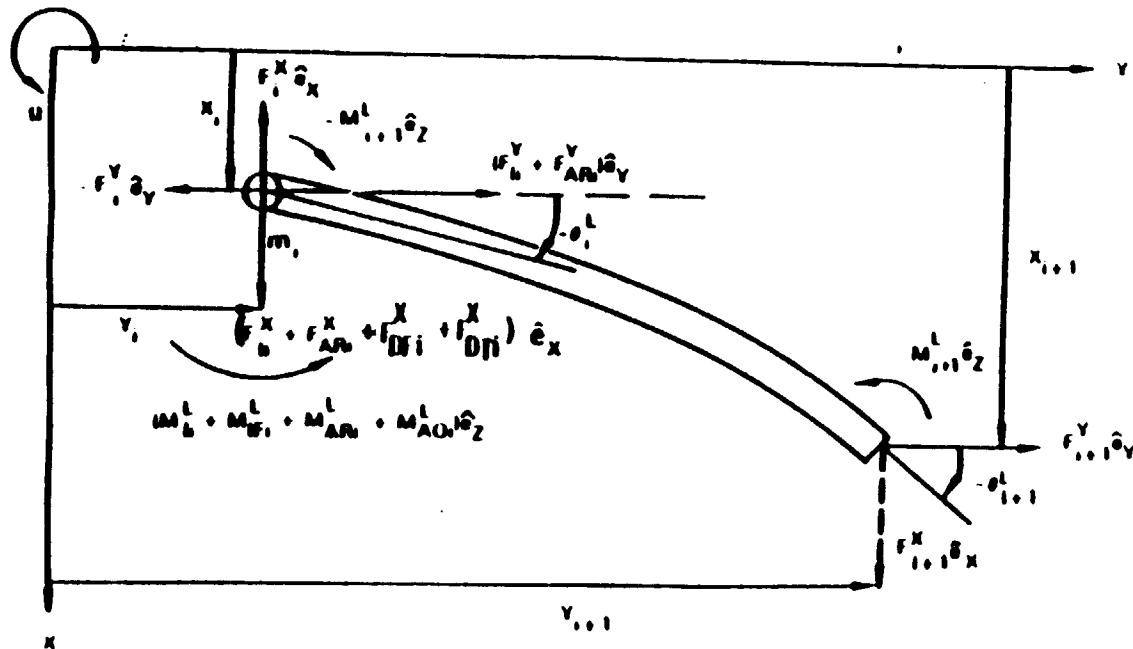
$$\begin{aligned}
 \text{FORCE EQUILIBRIUM:} \quad F_i^X &= F_I^X + F_{i+1}^X + F_{ARi}^X + F_{DTi}^X \\
 \text{MOMENT EQUILIBRIUM:} \quad M_i^L &= M_{i+1}^L + F_{i+1}^X(Y_{i+1} - Y_i) - F_{i+1}^Y(X_{i+1} - X_i) \\
 &\quad + M_{Ii}^L + M_{IFi}^L + M_{ARi}^L + M_{AOi}^L \\
 \text{X DISPLACEMENT:} \quad X_i &= X_{i+1} - \ell_{i,i+1} s \theta_i^L - X_{i+1\text{elastic}} - X_{i+1\text{kinematic}} \\
 \theta_i^L \text{ ROTATION:} \quad \theta_i^L &= \theta_{i+1}^L - \theta_{i+1\text{elastic}}^L - \theta_{i+1\text{built-in}}^L
 \end{aligned}$$

WHERE FOR STATION  $i$

- $F_I^X$  = INERTIA FORCE ,  $F_{AR}^Z$  = AERODYNAMIC FORCE
- $F_{DF}^X$  = AERODYNAMIC DAMPING FORCE DUE TO MOTION IN THE Z-DIRECTION
- $F_{DT}^X$  = AERODYNAMIC DAMPING FORCE DUE TO PITCHING MOTION
- $M_I^F$  = INERTIA MOMENT ABOUT THE Z-AXIS
- $M_{IF}^L$  = MOMENT OF THE INERTIA FORCES ABOUT THE Z-AXIS DUE TO CROSS SECTIONAL OFFSETS
- $M_{AR}^L$  = AERODYNAMIC MOMENT ABOUT THE Z-AXIS
- $M_{AO}^L$  = MOMENT ABOUT THE Z-AXIS OF THE AERODYNAMIC FORCES DUE TO SHEAR CENTER OFFSET FROM NEUTRAL-AXIS



## CHORDWISE EQUILIBRIUM AND COMPATIBILITY



Lead lag free body diagram for the  $i$ th blade element



---

### **6.3.3 TORSION EQUILIBRIUM AND COMPATIBILITY**

PRECEDING PAGE BLANK NOT FILMED

## TORSIONAL EQUILIBRIUM AND COMPATIBILITY

---

### TORSIONAL MOTION:

$$\begin{aligned}
 \text{RADIAL FORCE EQUILIBRIUM: } F_i^Y &= F_i^Y + F_{i+1}^Y + F_{ARi}^Y \\
 \text{MOMENT EQUILIBRIUM: } M_i^T &= M_{i+1}^T + M_{fi}^T + M_{ARi}^T + M_{AOi}^T + M_{DTi}^T + F_{i+1}^X \\
 &\quad (Z_{i+1} - Z_i) - F_{i+1}^Z (X_{i+1} - X_i) \\
 \text{Y DISPLACEMENT: } Y_i &= Y_{i+1} - \ell_{i,i+1} c \theta_i^F c \theta_i^L - Y_{i+1\text{elastic}} - Y_{i+1\text{kinematic}} \\
 \theta^T \text{ ROTATION: } \theta_i^T &= \theta_{i+1}^T - \theta_{i+1}^T \underset{\text{elastic}}{\quad} - \theta_{i+1}^T \underset{\text{built-in}}{\quad} - \theta_{input}^T
 \end{aligned}$$

where for  $i = \text{NHG1-1}$ ,  $\theta_{input}^T = \text{input pitch angle (collective, cyclic)}$

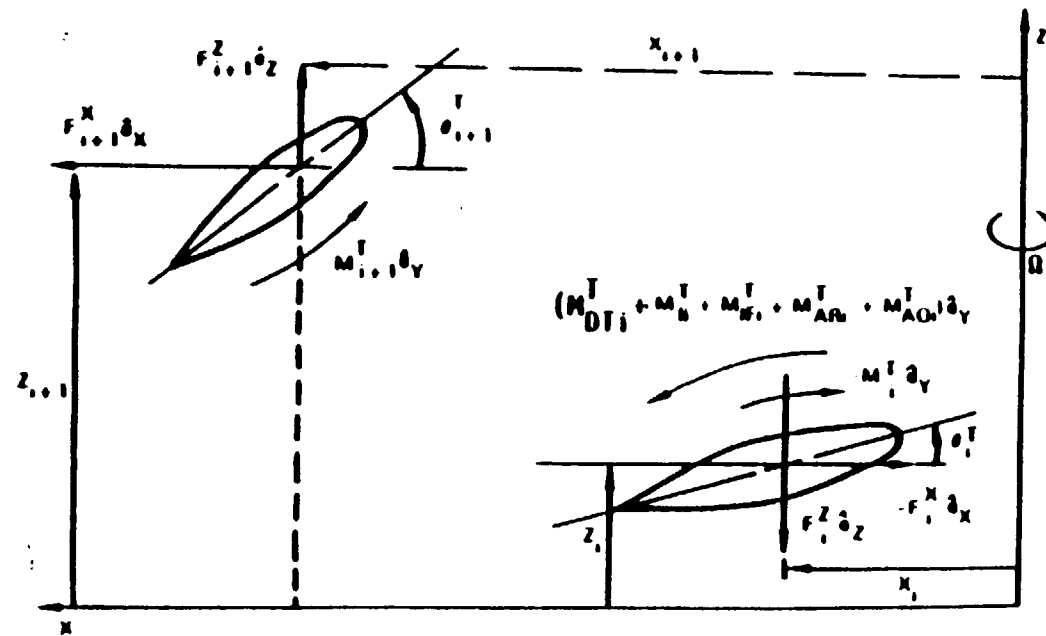
$i \neq \text{NHG1-1}$ ,  $\theta_{input}^T = 0$

and NHG1 is the station number giving the location of the torsion hinge

WHERE FOR STATION  $i$

$$\begin{aligned}
 F_Y^I &= \text{INERTIA FORCE,} & F_{AR}^Y &= \text{AERODYNAMIC FORCE} \\
 M_I^T &= \text{INERTIA MOMENT ABOUT THE Y-AXIS} \\
 M_{IF}^T &= \text{MOMENT OF THE INERTIA FORCES ABOUT THE Y-AXIS DUE TO CROSS} \\
 &\quad \text{SECTION OFFSETS BETWEEN SHEAR CENTER AND NEUTRAL AXIS} \\
 M_{AR}^T &= \text{AERODYNAMIC MOMENT ABOUT THE Y-AXIS} \\
 M_{AO}^T &= \text{MOMENT ABOUT THE Y-AXIS OF THE AERODYNAMIC FORCES DUE TO} \\
 &\quad \text{THE CROSS SECTIONAL OFFSETS BETWEEN SHEAR CENTER AND} \\
 &\quad \text{AERODYNAMIC CENTER} \\
 M_{DT}^T &= \text{MOMENT OF THE AERODYNAMIC DAMPING FORCE DUE TO PITCHING} \\
 &\quad \text{MOMENT}
 \end{aligned}$$

# TORSION EQUILIBRIUM AND COMPATIBILITY



Torsional free body diagram for the  $i$ th blade element.



---

## **6.4 BLADE CROSS SECTION DEFINITION**

PRECEDING PAGE BLANK NOT FILMED -

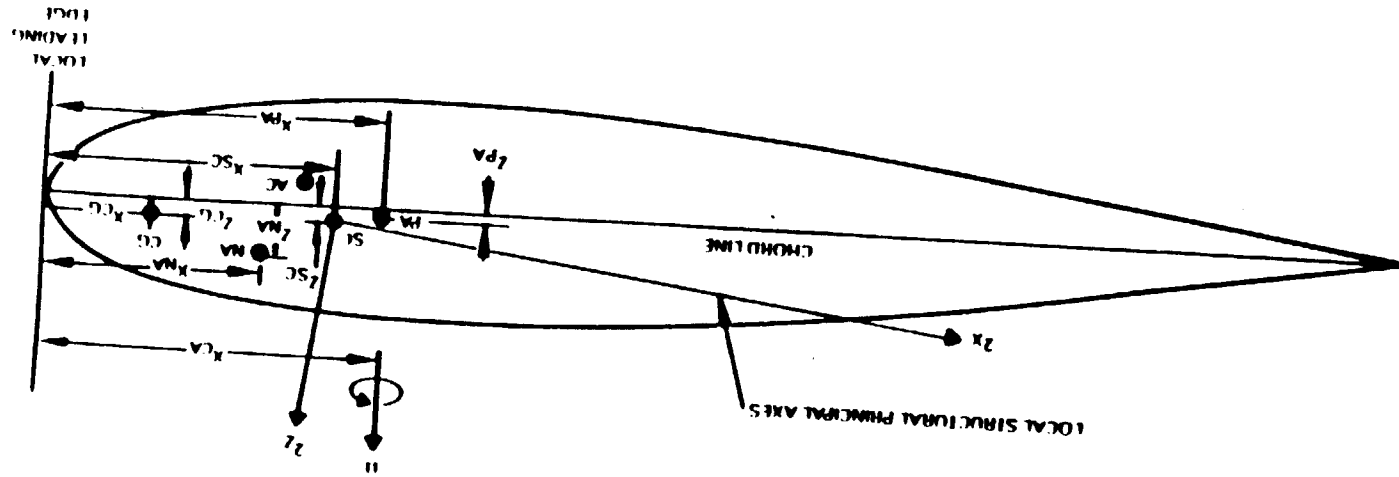
## **BLADE CROSS SECTION DEFINITION**

The blade cross section has been defined to provide a wide variety of variable parameters to enable the study of several different rotor cross sections. This includes:

1. Definition of distinct points for the beamwise and chordwise location of the shear center (SC), pitch axis (PA), center of gravity (CG), neutral axis (NA), and aerodynamic center (AC). At the blade root the PA is assumed to be coincident with the SC.
2. Arbitrary orientation of local structural principle axes (located at the SC).
3. Option to input center of rotation (CR) - pitch axis (PA) offset at the blade root (torque offset).



# BLADE CROSS SECTION DEFINITION





---

## **6.5 SPANWISE DISTRIBUTION OF STRUCTURAL, INERTIAL, AND GEOMETRIC PROPERTIES**

PRECEDING PAGE BLANK NOT FILMED

## **SPANWISE DISTRIBUTION OF STRUCTURAL, INERTIAL, AND GEOMETRIC PROPERTIES**

The transfer matrix method used for the rotor blade dynamic solution requires that the physical characteristics of the blade be specified at selected spanwise stations. RACAP implements a technique which uses blade distributed data per running inch of span length to determine the equivalent blade properties for the model. Equivalent inertia properties are calculated from mid-station to mid-station while equivalent structural and geometric properties are calculated from station to station.

## **SPANWISE DISTRIBUTION OF STRUCTURAL, INERTIAL, AND GEOMETRIC PROPERTIES**

---

- **EFFICIENT AND EASY TO IMPLEMENT PROCEDURE  
FOR GENERATING EQUIVALENT BLADE MODEL  
PROPERTIES FROM GIVEN DISTRIBUTED BLADE DATA**
- **EQUIVALENT INERTIA PROPERTIES CALCULATED  
FROM MID-STATION TO MID-STATION**
- **EQUIVALENT STRUCTURAL AND GEOMETRIC  
PROPERTIES CALCULATED FROM STATION TO  
STATION**



---

## **7.0    BLADE ROOT END MODELLING CAPABILITIES**

PRECEDING PAGE BLANK NOT FILMED





---

## 7.1 ARTICULATED ROTORS

PRECEDING PAGE IN ARK NOT FILMED

## ARTICULATED ROTORS

Articulated rotors with arbitrary hinge sequence can be modeled in RACAP. This includes configurations with coincident and noncoincident hinges and also arbitrary sequencing of the root hinges. At each hinge location, provision for kinematic coupling of the hinge degree-of-freedom with the other two degrees of freedom can be incorporated. Geometric blade properties such as precone, twist, droop, and sweep can be included in the model formulation.

## **ARTICULATED ROTORS**

---

- **COINCIDENT AND NON-COINCIDENT HINGES**
- **ARBITRARY SEQUENCING OF ROOT HINGES**
- **PROVISION FOR KINEMATIC COUPLING AT HINGE LOCATIONS**
- **INCLUSION OF GEOMETRIC BLADE PROPERTIES SUCH AS PRECONE, DROOP, SWEEP, ETC.**



---

## **7.2 TEETERING ROTORS**

## TEETERING ROTORS

Teetering rotors with geometric blade properties such as precone, undersling, built-in-twist, etc. can be modeled in a straightforward manner in RACAP. Provisions for including root end kinematic couplings such as flap-pitch or pitch-lag coupling are included. A special feature of RACAP is that it lends itself well to the treatment of the teetering rotor root boundary conditions. Since the solution is formulated in the frequency domain, the root boundary conditions are cantilevered for the steady state and even harmonics and pinned for the odd harmonics of the blade motion.

## **TEETERING ROTORS**

---

- **PROVISION FOR INCLUDING UNDERSLING, PRECONE, DROOP.**
- **CONSIDERATION OF ROOT END KINEMATIC COUPLINGS**
- **SIMPLIFIED TREATMENT OF BOUNDARY CONDITIONS DUE TO CHOICE OF FREQUENCY DOMAIN SOLUTION: STEADY STATE AND EVEN HARMONICS MODELED WITH CANTILEVERED BOUNDARY, ODD HARMONICS MODELED WITH PINNED BOUNDARY**





PRECEDING PAGE BLANK NOT FILMED

---

## **7.3 HINGELESS/BEARINGLESS ROTORS**

## **HINGELESS/BEARINGLESS ROTORS**

The unique root configurations associated with hingeless and bearingless rotors can be modeled in RACAP. For the hingeless rotor, precone, droop, and kinematic coupling at the feathering hinge can be provided. Inclusion of hub static stiffness and dynamic impedance characteristics coupled with the rotor model provide a comprehensive hingeless rotor system model for the RACAP analysis. For bearingless rotors the RACAP model incorporates the multiple load paths, the effects of moderate deformations due to bending, and compatibility at the outboard and inboard interface between the flexbeam, pitch case, and blade.

## **HINGELESS/BEARINGLESS ROTORS**

---

- **HINGELESS ROTORS**
  - **GEOMETRIC PROPERTIES SUCH AS PRECONE, DROOP.**
  - **KINEMATIC COUPLING AT THE FEATHERING HINGE**
- **BEARINGLESS ROTORS**
  - **REDUNDANT LOAD PATHS**
  - **MODERATE DEFLECTIONS DUE TO BENDING**
  - **COMPATIBILITY AT INTERFACE**



---

## **8.0 BLADE FORCED RESPONSE TRANSFER MATRIX SOLUTION TECHNIQUE**

PRECEDING PAGE BLANK NOT FILMED



---

## **8.1 BLADE ELEMENT TRANSFER MATRIX MODEL**

PRECEDING PAGE BLANK NOT FILMED

## BLADE ELEMENT TRANSFER MATRIX MODEL

A transfer matrix method which is based on a fully coupled flap-lag-torsion structural model is used to discretize the equations of motion for the solution of the rotor blade dynamics problems. This method is classified as a hybrid discrete element dynamic analysis procedure. Since both displacement and force quantities are retained as unknowns, the blade load distribution is directly obtained as part of the aeroelastic response. The transfer matrix state vector at any particular station  $i$  consists of twelve state variables defined with respect to the rotating hub-fixed coordinate system.

The transfer relations from station  $i$  to an adjacent station  $i + 1$  are obtained by formulating equations of force and moment equilibrium and displacement and rotation compatibility between the two stations. All equations are derived in the hub-fixed coordinate system. The resulting equations are nonlinear. These equations are linearized about a previously known solution for the steady (azimuth independent in the rotating system) equilibrium position and about the converged steady equilibrium position solution for the direct harmonic perturbation solution. The steady equilibrium position is found by a relaxation technique, wherein incremental linearized equations are derived from the last iteration of the structural response. The solution to the incremental equations is added to the previous iteration solution, and the process repeated until a converged solution is finally obtained. The harmonic solution is obtained as a direct solution of the harmonic incremental equations, linearized about the converged steady solution.



## **BLADE ELEMENT TRANSFER MATRIX MODEL**

---

- **FULLY COUPLED FLAP-LAG-TORSION MODEL**
- **HYBRID FORCE-DISPLACEMENT FORMULATION**
- **EQUATIONS OF EQUILIBRIUM AND COMPATIBILITY ARE SOLVED IN HUB-FIXED GLOBAL FRAME**
- **HARMONIC SOLUTION IS ABOUT THE STEADY EQUILIBRIUM POSITION**
- **DIRECT HARMONIC BALANCE SOLUTION**



---

## 8.2 BLADE TRANSFER MATRIX RELATIONS

PRECEDING PAGE BLANK NOT FILMED

## BLADE TRANSFER MATRIX RELATIONSHIPS

Before the transfer matrix solution procedure can be implemented three important transfer matrix relationships must be established for the rotor blade model. These are:

1. The field transfer relationships which relate state variables in a continuous span of the blade (e.g., the relation of the state variables an infinitesimal distance to the left of the blade tip to the state variables an infinitesimal distance to the right of the outermost hinge, lead-lag in following example).
2. The point transfer relationships which relate state variables over a discontinuity such as a hinge location in the blade span (e.g., the relation of the state variables to the left of the lead-lag hinge with those to the right of the lead-lag hinge).
3. The hinge equilibrium equations expressed in terms of the discontinuities at the hinge and the displacement and rotation state variables at the blade tip.

After these relationships have been developed, the transfer matrix method solution technique can be formulated either as an iterative procedure for the solution of the steady equilibrium position or as a direct solution for the harmonic response.

## BLADE ELEMENT TRANSFER MATRIX MODEL

---

- **BLADE STRUCTURAL MODEL IS FULLY COUPLED IN FLAP, LEAD-LAG, AND TORSION**

$$\{\Delta \vec{Z}\}_i = [M_1(\vec{Z}_i)]\{\Delta \vec{Z}\}_{i+1} + \{M_2(\vec{Z}_i, others)\}$$

where

$$\{\Delta \vec{Z}\}_i^T = \{\Delta M^F, \Delta \theta^F, \Delta F^Z, \Delta Z, \Delta M^T, \Delta \theta^T, \Delta F^Y, \Delta Y, \Delta M^L, \Delta \theta^L, \Delta F^X, \Delta X\}_i$$

AND  $\{\vec{Z}_i\}$  REPRESENTS THE PREVIOUS ITERATION VALUE OF THE STATE VECTOR IN THE STEADY STATE SOLUTION AND THE CONVERGED STEADY STATE RESPONSE IN THE DYNAMIC PERTURBATION SOLUTION



## BLADE TRANSFER MATRIX RELATIONSHIPS

---

H0
H1
H2
N+1  
 FLAP    TORSION    LEAD-LAG

### • TRANSFER RELATIONSHIPS

$$\{\Delta \vec{Z}\}_{H2}^R = [d]\{\Delta \vec{Z}\}_{n+1} + \{\alpha\} \quad (1)$$

$$\{\Delta \vec{Z}\}_{H1}^R = [U^{12}]\{\Delta \vec{Z}\}_{H2}^L + \{\alpha^{12}\} \quad (2)$$

$$\{\Delta \vec{Z}\}_{H0}^R = [U^{01}]\{\Delta \vec{Z}\}_{H1}^L + \{\alpha^{01}\} \quad (3)$$

### • DISCONTINUITY EQUATIONS

$$\{\Delta \vec{Z}\}_{H2}^L = [H2]\{\Delta \vec{Z}\}_{H2}^R - \{r^{H2}\}(\Delta \theta H2) \quad (4)$$

$$\{\Delta \vec{Z}\}_{H1}^L = [H1]\{\Delta \vec{Z}\}_{H1}^R - \{r^{H1}\}(\Delta \theta H1) \quad (5)$$

WHERE [H1] AND [H2] ARE KINEMATIC COUPLING MATRICES  
 AND  $\Delta \theta H2$  and  $\Delta \theta H1$  ARE THE LOCAL ANGLE DISCONTINUITIES  
 AT THE HINGES





## BLADE TRANSFER MATRIX RELATIONSHIPS (continued)

---

### • HINGE EQUILIBRIUM EQUATIONS

$$[M_3]\{\Delta\vec{Z}^*\}_{N+1} + [M_4]\{\Delta\theta_D\} + [M_5] = 0 \quad (6)$$

WHERE

$$\{\Delta\vec{Z}^*\}_{N+1}^T = \{\Delta\theta^F, \Delta Z, \Delta\theta^T, \Delta Y, \Delta\theta^L, \Delta X\}_{N+1}$$

COMBINING EQUATIONS (1) THROUGH (6) RESULTS IN THE FORMULATION FOR THE ITERATIVE ALGORITHM OF THE STEADY STATE SOLUTION OR THE DIRECT SOLUTION OF THE HARMONIC PERTURBATION MOTION



# COUPLED ROTOR/AIRFRAME FORCED RESPONSE

(continued)

---

- SOLUTION FOR COUPLED ROTOR/AIRFRAME N-1, N, N+1 HARMONIC PERTURBATION TIP DISPLACEMENTS AND HINGE DISCONTINUITY ANGLES (CONTD)
- EQUATIONS (7) AND (14) RESULT IN

$$[E_{OCH}]\{\tilde{\eta}_{TCH}^P\} + [e_{OCH}]\{\tilde{\eta}_{DCH}^P\} + \{\tilde{\alpha}_{EOCH}\} = \{0\} \quad (15)$$

where

$$[E_{OCH}] = [B_{OCH}] - [\gamma][R][\lambda][C_{OCH}] \quad (16)$$

$$[e_{OCH}] = [b_{OCH}] - [\gamma][R][\lambda][c_{OCH}] - [CRB] \quad (17)$$

$$[\tilde{\alpha}_{EOCH}] = \{\tilde{\alpha}_{\eta OCH}\} - [\gamma][R][\lambda]\{\tilde{\alpha}_{FOCH}\} \quad (18)$$

- COMBINE EQUATIONS (12) AND (15) TO YIELD THE SOLUTION

$$\begin{Bmatrix} \{\tilde{\eta}_{TCH}^P\} \\ \{\tilde{\eta}_{DCH}^P\} \end{Bmatrix} = -[A_{OCH}]^{-1}\{\tilde{\alpha}_{AOCH}\} \quad (19)$$

where

$$[A_{OCH}] = \begin{bmatrix} [E_{OCH}] & [e_{OCH}] \\ [D_{OCH}] & [d_{OCH}] \end{bmatrix} \quad (20)$$

and

$$\{\tilde{\alpha}_{AOCH}\} = \begin{Bmatrix} \{\tilde{\alpha}_{EOCH}\} \\ \{\tilde{\alpha}_{DOCH}\} \end{Bmatrix} \quad (21)$$

THE REMAINING BLADE STATE VARIABLES ARE OBTAINED BY  
MULTIPLYING THE TRANSFER MATRICES PROCEEDING FROM TIP TO ROOT



---

## **9.0 COUPLED ROTOR/AIRFRAME FORCED RESPONSE FORMULATION**

PRELIMINARY PAGE. BLANK NOT FILMED



---

## **9.1 OVERALL APPROACH**

## OVERALL APPROACH

The approach used in RACAP for the determination of coupled rotor/airframe response is the impedance matching procedure. The rotor impedance is (implicitly) calculated using the transfer matrix method. Airframe impedance is computed using NASTRAN. The forces and displacements at the hub are matched to yield the proper coupling relations between rotor and airframe. The advantage of using impedance matching at the hub is that the rotor impedance can be obtained considering only one blade. It is assumed that all blades of the rotor experience the same loading at the same azimuth position. Since the analysis is performed in the frequency domain the response is obtained by a superposition of the harmonic responses.



## OVERALL APPROACH

---

- DETERMINED USING THE IMPEDANCE MATCHING TECHNIQUE
  - CALCULATION OF ROTOR IMPEDANCE
  - DETERMINATION OF AIRFRAME IMPEDANCE
  - MATCHING OF FORCES AND DISPLACEMENTS AT THE HUB
- ADVANTAGE IN THAT ROTOR IMPEDANCE CAN BE OBTAINED BY CONSIDERING A SINGLE BLADE
- ASSUMPTION INHERENT IN USING IMPEDANCE MATCHING:
  - ALL BLADES OF THE ROTOR EXPERIENCE THE SAME LOADING AT THE SAME AZIMUTH POSITION
- RESULTANT RESPONSE IS OBTAINED BY A SUPERPOSITION OF HARMONIC PERTURBUATION RESPONSES



---

## 9.2 SOLUTION TECHNIQUE



---

### **9.2.1 ROTOR IMPEDANCE FORMULATION**

PRECEDING PAGE BLANK NOT FILMED

## ROTOR IMPEDANCE FORMULATION

In order to determine the coupled rotor/airframe response the rotor impedance must be obtained. This consists of formulating expressions for the blade root displacements and forces in terms of the unknown tip displacements and the angular discontinuities at the hinges.

## ROTOR IMPEDANCE FORMULATION

---

- DETERMINATION OF HARMONIC PERTURBATION BLADE ROOT DISPLACEMENTS AND FORCES IN TERMS OF PERTURBATION UNKNOWN TIP DISPLACEMENTS AND UNKNOWN HINGE ANGULAR DISCONTINUITIES

$$\{\tilde{\eta}_{ON}^P\} = [B_{ON}]\{\tilde{\eta}_{TN}^P\} + [b_{ON}]\{\tilde{\eta}_{DN}^P\} + \{\tilde{\alpha}_{NON}\} \quad (7)$$

$$\{\tilde{F}_{ON}^P\} = [C_{ON}]\{\tilde{\eta}_{TN}^P\} + [c_{ON}]\{\tilde{\eta}_{DN}^P\} + \{\tilde{\alpha}_{FON}\} \quad (8)$$





---

## **9.2.2 AIRFRAME IMPEDANCE CALCULATION**

## AIRFRAME IMPEDANCE CALCULATION

A NASTRAN finite element model is used to determine the airframe hub mobility. Unit vibratory forces and moments are applied to the hub at N/REV in fixed coordinates and the resulting forced hub response constitutes the elements of the 6x6 complex response matrix [R] (inverse of the impedance).

## AIRFRAME IMPEDANCE CALCULATION

---

- CALCULATION OF AIRFRAME RESPONSE

$$\{\vec{Z}_F\} = [R]\{\vec{S}_F\}$$

WHERE THE RESPONSE MATRIX  $[R]$  IS DETERMINED FROM NASTRAN BY APPLYING UNIT VIBRATION FORCES AND MOMENTS TO THE ROTOR HUB AT N/REV IN THE FIXED COORDINATE SYSTEM



---

### **9.2.3 RELATIONSHIP OF ROTATING AND FIXED SYSTEM DISPLACEMENTS AND FORCES**

PRECEDING PAGE BLANK NOT FILMED

## RELATIONSHIP OF ROTATING AND FIXED SYSTEM DISPLACEMENTS AND FORCES

The relationship between the rotating and fixed system displacements and forces at the blade root are required in the process of determining coupled rotor/airframe response. Displacements and rotations in the rotating and fixed systems are related by considering compatibility requirements at the blade root. Forces and moments in the rotating and fixed systems are related by considering equilibrium of the individual harmonics in the fixed system. This results in the expressions which contain  $N-1$ ,  $N$ ,  $N+1$  harmonics of the rotating system related to  $N/\text{REV}$  harmonics in the fixed system, (since  $N/\text{REV}$  forces in the fixed system determine the fuselage response).

## RELATIONSHIP OF ROTATING AND FIXED SYSTEM DISPLACEMENTS AND FORCES

---

- DERIVATION OF COUPLING RELATIONSHIPS FOR  
ROTATING AND NON-ROTATING DISPLACEMENTS AND  
FORCES AT THE BLADE ROOT

DISPLACEMENTS:  $\{\vec{\eta}_{OCH}^P\} = [\gamma]\{\vec{Z}_F\} + \{\eta_D^{FP}\}$  (10)

FORCES:  $\{\vec{S}_F\} = [\lambda]\{\vec{F}_{OCH}^P\}$  (11)





---

## **9.2.4 INBOARD HINGE MOMENT EQUILIBRIUM EQUATIONS**

## **INBOARD HINGE MOMENT EQUILIBRIUM EQUATIONS**

Moment equilibrium equations at the hinges are required for the  $N-1$ ,  $N$ , and  $N+1$  harmonics. These equilibrium equations are expressed in terms of the harmonic tip state vector displacements and rotations and the harmonic discontinuities in the angles across the hinges.

## INBOARD HINGE MOMENT EQUILIBRIUM EQUATIONS

---

- **MOMENT EQUILIBRIUM EQUATIONS AT HINGES IN TERMS OF TIP DISPLACEMENTS AND DISCONTINUITIES ACROSS THE HINGES**

$$[D_{OCH}]\{\vec{\eta}_{TCH}^P\} + [d_{OCH}]\{\vec{\eta}_{DCH}^P\} + \{\vec{\alpha}_{DOCH}\} = \{0\} \quad (12)$$



PRECEDING PAGE BLANK NOT FILMED

---

### **9.2.5 BOUNDARY CONDITION FORMULATION USING HARMONIC ANALYSIS APPROACH**

## **BOUNDARY CONDITION FORMULATION USING HARMONIC ANALYSIS APPROACH**

Using the frequency domain-harmonic analysis approach enables a clear distinction and straightforward formulation of the boundary conditions required for the solution of the coupled rotor/airframe response problem. For the steady equilibrium position solution, the rotor hub is considered to be rigid. For an  $N$ -bladed rotor the  $N-1$ ,  $N$ , and  $N+1$  harmonics are coupled with the airframe using impedance matching. The remaining harmonics are assumed to be uncoupled from the airframe motion and are solved for separately.

## BOUNDARY CONDITION FORMULATION USING HARMONIC ANALYSIS APPROACH

---

- STEADY STATE SOLUTION IS DETERMINED USING AN ITERATIVE APPROACH ASSUMING A RIGID ROTOR HUB
- $(N-1)$ ,  $N$ ,  $(N+1)$  HARMONIC ( $N$ = NUMBER OF ROTOR BLADES) SOLUTION COUPLED WITH AIRFRAME
- OTHER HARMONICS UNCOUPLED <sup>FROM</sup> AIRFRAME MOTION





---

## **9.3 COUPLED ROTOR/AIRFRAME FORCED RESPONSE**

## COUPLED ROTOR/AIRFRAME FORCED RESPONSE

The solution for the coupled rotor/airframe forced response is obtained in a four-step procedure:

1. The  $N-1$ ,  $N$ , and  $N+1$  harmonic rotating root displacements are expressed in terms of the displacement and force rotating-to-nonrotating transformation matrices,  $[\gamma]$  and  $[\lambda]$ , respectively, the NASTRAN response matrix  $[R]$ , and the  $N-1$ ,  $N$ , and  $N+1$  harmonic rotating blade root forces (Equation (13)).
2. The expression for the  $N-1$ ,  $N$  and  $N+1$  harmonic rotating blade root forces (Equation (8)), which is in terms of the harmonic blade tip displacements and rotations and hinge angular discontinuities, is substituted into the expression for the  $N-1$ ,  $N$ , and  $N+1$  harmonic rotating root displacements in 1) above. This results in the  $N-1$ ,  $N$ , and  $N+1$  rotating root displacements expressed in terms of the  $N-1$ ,  $N$ , and  $N+1$  harmonic tip displacements and hinge angular discontinuities (Equations (14)).

## COUPLED ROTOR/AIRFRAME FORCED RESPONSE

---

- SOLUTION FOR COUPLED ROTOR/AIRFRAME N-1, N, N+1 HARMONIC PERTURBATION TIP DISPLACEMENTS AND HINGE DISCONTINUITY ANGLES
- COMBINING EQUATIONS (9), (10), and (11)

$$\{\tilde{\eta}_{OCH}^P\} = [\gamma][R][\lambda]\{F_{OCH}^P\} + \{\tilde{\eta}_D^{FP}\} \quad (13)$$

- SUBSTITUTE FOR THE ROTATING VECTOR  $\{\tilde{F}_{OCH}^P\}$  FROM EQUATION (8)

$$\begin{aligned} \{\tilde{\eta}_{OCH}^P\} = & [\gamma][R][\lambda][C_{OCH}]\{\tilde{\eta}_{TCH}^P\} + [\gamma][R][\lambda][C_{OCH}]\{\eta_{TCH}^D\} \\ & + [\gamma][R][\lambda]\{\tilde{\alpha}_{FOCH}\} + \{\tilde{\eta}_D^{FP}\} \end{aligned} \quad (14)$$

### COUPLED ROTOR/AIRFRAME FORCED RESPONSE (continued)

- 3) The expressions (Equations (7) and (14)) for  $N-1$ ,  $N$ , and  $N+1$  rotating root displacements expressed in terms of the  $N-1$ ,  $N$ , and  $N+1$  harmonic tip displacements and hinge discontinuities are equated.
- 4) The resulting equation (Equation (15)) is combined with the  $N-1$ ,  $N$ , and  $N+1$  moment equilibrium equations at the hinges (Equation (12)) to yield the matrix equation (Equation (19)) which can be directly solved to determine the  $N-1$ ,  $N$ , and  $N+1$  harmonic tip displacements and rotations and hinge discontinuity angles.

In order to determine the remaining  $N-1$ ,  $N$ , and  $N+1$  state variables along the blade span, the element transfer matrices and discontinuity relations are multiplied proceeding from blade tip to root.

## COUPLED ROTOR/AIRFRAME FORCED RESPONSE

(continued)

- SOLUTION FOR COUPLED ROTOR/AIRFRAME N-1, N, N+1 HARMONIC PERTURBATION TIP DISPLACEMENTS AND HINGE DISCONTINUITY ANGLES (CONTD)

- EQUATIONS (7) AND (14) RESULT IN

$$[E_{OCH}]\{\tilde{\eta}_{TCH}^P\} + [e_{OCH}]\{\tilde{\eta}_{DCH}^P\} + \{\tilde{\alpha}_{EOCH}\} = \{0\} \quad (15)$$

where

$$[E_{OCH}] = [B_{OCH}] - [\gamma][R][\lambda][C_{OCH}] \quad (16)$$

$$[e_{OCH}] = [b_{OCH}] - [\gamma][R][\lambda][c_{OCH}] - [CRB] \quad (17)$$

$$[\tilde{\alpha}_{EOCH}] = \{\tilde{\alpha}_{\eta OCH}\} - [\gamma][R][\lambda]\{\tilde{\alpha}_{FOCH}\} \quad (18)$$

- COMBINE EQUATIONS (12) AND (15) TO YIELD THE SOLUTION

$$\begin{Bmatrix} \{\tilde{\eta}_{TCH}^P\} \\ \{\tilde{\eta}_{DCH}^P\} \end{Bmatrix} = -[A_{OCH}]^{-1}\{\tilde{\alpha}_{AOCH}\} \quad (19)$$

where

$$[A_{OCH}] = \begin{bmatrix} [E_{OCH}] & [e_{OCH}] \\ [D_{OCH}] & [d_{OCH}] \end{bmatrix} \quad (20)$$

and

$$\{\tilde{\alpha}_{AOCH}\} = \begin{Bmatrix} \{\tilde{\alpha}_{EOCH}\} \\ \{\tilde{\alpha}_{DOCH}\} \end{Bmatrix} \quad (21)$$

THE REMAINING BLADE STATE VARIABLES ARE OBTAINED BY  
MULTIPLYING THE TRANSFER MATRICES PROCEEDING FROM TIP TO ROOT



---

**10. ANALYSIS AND CORRELATION PLAN**

The analysis and correlation plan is designed to follow four steps.

- (i) Derivation of AH-1G-specific blade constraints such as even and odd harmonic boundary conditions and effects of precone and underslinging.
- (ii) Programming of the AH-1G model and verification of the structural model by conducting a forced response frequency sweep to identify all modes of the blade model.
- (iii) Verification of the finite element structural model by conducting several checks on the fuselage finite element grid.
- (iv) Defining and integrating the aerodynamic model for the AH-1G teetering rotor with the structural model to compute the aeroelastic response in a single modular program.

The complete RACAP formulation will be exercised at a specific flight condition (114 knots) to identify modeling errors by performing correlation studies on airloads and blade loads (via test measurements). Satisfactory correlation will be obtained at 114 knots prior to analysis at other flight conditions.



## **ANALYSIS AND CORRELATION PLAN**

---

- **DERIVE BLADE STRUCTURAL MODEL**
- **VERIFY BLADE STRUCTURAL MODEL THROUGH MODAL SURVEY**
- **VERIFY FUSELAGE FINITE ELEMENT MODEL**
- **DEFINE AND INTEGRATE AERODYNAMIC MODEL IN RACAP**
- **CORRELATE RACAP AND TEST DATA FOR ONE FLIGHT CONDITION (114 KNOTS)**
- **PERFORMANCE ANALYSIS AT OTHER FLIGHT CONDITIONS**



---

## **10.1 AH-1G BLADE STRUCTURAL MODELING**

PRECEDING PAGE BLANK NOT FILMED

## **AH-1G BLADE STRUCTURAL MODELING**

In the frequency domain, where a single blade is modeled to simulate an entire rotors' response, the teetering rotor is modeled using different boundary conditions for even and odd harmonics. These are, cantilevered for even, and pinned for odd. The model includes underslinging and preconing effects. The lag hinge is absent, while the control system is modeled by a single spring. The model is limited by the assumptions listed below.

- Fuselage vibrations are uninfluenced by control system/aerodynamic interaction.
- The fuselage FEM is linear.
- The elastomeric "soft" transmission support is independent of frequency.
- The higher frequency vibrations are not calculated ( $> 2$  rev).

## **AH-1G BLADE STRUCTURAL MODELING**

---

- **MODEL EVEN AND ODD HARMONIC BOUNDARY CONDITIONS INDIVIDUALLY**
- **INCLUDE UNDERSLINGING AND PRECONE EFFECTS**
- **LAG HINGE - ABSENT**
- **CONTROL SYSTEM MODELED BY SINGLE SPRING**

### **ASSUMPTIONS**

- **FUSELAGE VIBRATION THROUGH CONTROL SYSTEM AND AERODYNAMIC INTERACTION NEGLECTED**
- **NON LINEARITIES OF FUSELAGE MODEL NEGLECTED**
- **LIMITED ACCESS TO PROPERTIES OF "SOFT" TRANSMISSION SUPPORT**
- **FUSELAGE VIBRATION PREDICTED AT 2/REV (4/REV, 6/REV NEGLECTED)**



---

## **10.2 AH-1G AERODYNAMICS MODEL**

## AH-1G AERODYNAMICS MODEL

An isolated rotor trim program was used to define the rigid blade airloads using (a) Glauert inflow and (b) a free wake inflow model. Both analyses used a blade element analysis (lifting line model) and experimentally measured 2-D airfoil data. Airloads correlations with flight test data were done with both inflow models. The free wake model was adopted for the remaining analysis because it yielded better correlation with measured airloads.



## **AH-1G AERODYNAMICS MODEL**

---

- **ISOLATED ROTOR TRIM**
- **GLAUERT/FREE WAKE INFLOW MODEL**
- **RIGID BLADE ANALYSIS**
- **BLADE ELEMENT ANALYSIS**
- **EXPERIMENTALLY MEASURED STEADY 2D AIRFOIL DATA**



---

## 10.3 AH-1G AIRFRAME MODEL

## AH-1G AIRFRAME MODEL

Several checks were conducted on the fuselage finite element model to ensure its validity. These were, (i) the multi-level strain energy check, (ii) kinetic energy check, (iii) connectivity check. In the multi-level strain energy check, the strain energy of the free-free model are calculated and used to identify errors in modelling in the "G", "N", "F" set levels. In the kinetic energy check, global and local structural modes can be identified with computational ease and speed. The connectivity check identifies areas of singularity in the model due to misaligned or incomplete connectivities in the model.

The hub impedance matrix (at 2/Rev) is used in arriving at coupled rotor-fuselage hub loads. This matrix was calculated using the airframe NASTRAN model, employing a modal response solution sequence. Transfer matrices (at 2/Rev) relating unit hub loads to vibrations at locations of interest on the fuselage are generated using the same airframe model and modal response solution.

## **AH-1G AIRFRAME MODEL**

---

- **CHECKS CONDUCTED ON AH-1G FEM:**
  - **MULTI-LEVEL STRAIN ENERGY**
  - **KINETIC ENERGY**
  - **CONNECTIVITY**
- **HUB IMPEDANCE MATRIX GENERATED AT 2 REV  
(MODAL RESPONSE SOLUTION)**
- **FUSELAGE VIBRATION RESPONSE MATRICES  
GENERATED AT 2P (MODAL RESPONSE SOLUTION)**



---

## **10.4 COUPLED ROTOR-FUSELAGE ANALYSIS**

## COUPLED ROTOR-FUSELAGE ANALYSIS

The coupled rotor-fuselage procedure was described in detail earlier for a generic helicopter. For the AH-1G, the matched impedance method is applied to the 1, 2, and 3 harmonics of rotor RPM. All other harmonics up to 9 are modelled with a rigid hub (i.e. uncoupled from the fuselage motions). This assumption makes use of the fact that the rotor acts as a frequency filter and transmits only loads at integral multiples of the blade passage frequency to the fuselage. The hub loads obtained in the rotating system are transformed to the fixed system at blade passage frequency and are then used with the fuselage transfer matrices to compute the fuselage vibration response at locations of interest.



## **COUPLED ROTOR-FUSELAGE ANALYSIS**

---

- **AIRFRAME HUB IMPEDANCE FROM FEM MATCHED WITH ROTOR HUB IMPEDANCE**
- **1, 2, 3, HARMONICS ANALYSIS PERFORMED WITH FUSELAGE COUPLING**
- **ALL OTHER HARMONICS (UP TO 9) ARE UNCOUPLED FROM FUSELAGE**
- **2P HUB LOADS (IN FIXED SYSTEM) APPLIED TO FUSELAGE RESPONSE MATRICES FOR VIBRATION LEVEL CORRELATION**



---

## **11.0 DISCUSSION OF RESULTS**

## DISCUSSION OF RESULTS

Fuselage acceleration levels (lateral and vertical) for all flight conditions (steady forward flight, 67 to 142 knots) compare favorably. Some general trends are identified below.

(a) Vertical vibration prediction is generally better correlated than lateral vibration predictions. This trend is consistent with the results of the study of the finite element model and the test data (Appendix 1). Those results indicate a factor of six discrepancy between calculated (derived from measured mast top accelerations at 85 knots) and measured lateral acceleration values at the nose. In that study, the vertical vibration levels are much more consistent than the lateral. RACAP predictions and measured vibration levels show a discrepancy of about a factor of 6.5 in the lateral hub vibration prediction at 85 knots. This discrepancy feeds into the vibration prediction at any given location on the ship in the lateral direction. However, the problem appears to lie in the finite-element formulation rather than the load prediction methodology. In Appendix 1, the fuselage finite element model effectively has a higher impedance at 2P than is realistic. This manifests itself in two ways: (i) the root boundary conditions are overly stiff and therefore the hub loads are magnified; and (ii) for a given hub load the fuselage accelerations are underestimated. Of these, the magnification of coupled rotor-fuselage hub loads is probably more pronounced due to the strong dependence of the response on the fuselage impedance. Insofar as this behavior is more pronounced in the lateral direction, correlation of fuselage acceleration in that direction is expected to be poorer than the vertical, although the latter is also affected.

(b) Lower speed flight conditions generally show better correlation than higher speed conditions at the same location.

The nonlinearity of the elastomeric mounts is not adequately characterized in the longitudinal/lateral directions. The nonlinear stiffness and damping of the mounts varies with load magnitude; this effect is not included in the transfer matrix formulation. At higher flight speeds, the hub impedance matrix defining the root boundary conditions would also be changed by the inclusion of this effects. Hence the inconsistency.

(c) Forward locations on the ship indicate better correlation than aft locations.

A major influence on aft location vibrations is the 2P main rotor wake impinging on the aft fuselage. These loads are not a part of RACAP formulation. Since these loads are not calculated in the present formulation, the influence of this effect on the vibratory response is not accounted for. In addition, 2P control system link loads have an influence on the fuselage vibrations that are not part of this analysis. These vibration predictions may have been improved by the inclusion of these effects.

## **DISCUSSION OF RESULTS**

---

- **VERTICAL FUSELAGE VIBRATION LEVELS AFFORD GOOD CORRELATION WITH MEASURED DATA IN FORWARD PART OF SHIP**
- **AFT VERTICAL VIBRATION CORRELATION NOT AS GOOD DUE TO MISSING EMPENNAGE ROTOR WAKE EXCITATION**
- **LATERAL VIBRATION RESPONSE CORRELATION NOT AS GOOD AS VERTICAL VIBRATION LEVEL CORRELATION**
- **FUSELAGE FEM NEEDS REFINEMENT – CHECK NOT SATISFACTORILY CONSISTENT (REF. APPENDIX 1)**



---

## 11.1 RESULTS

PRECEDING PAGE BLANK NOT FILMED

## RESULTS

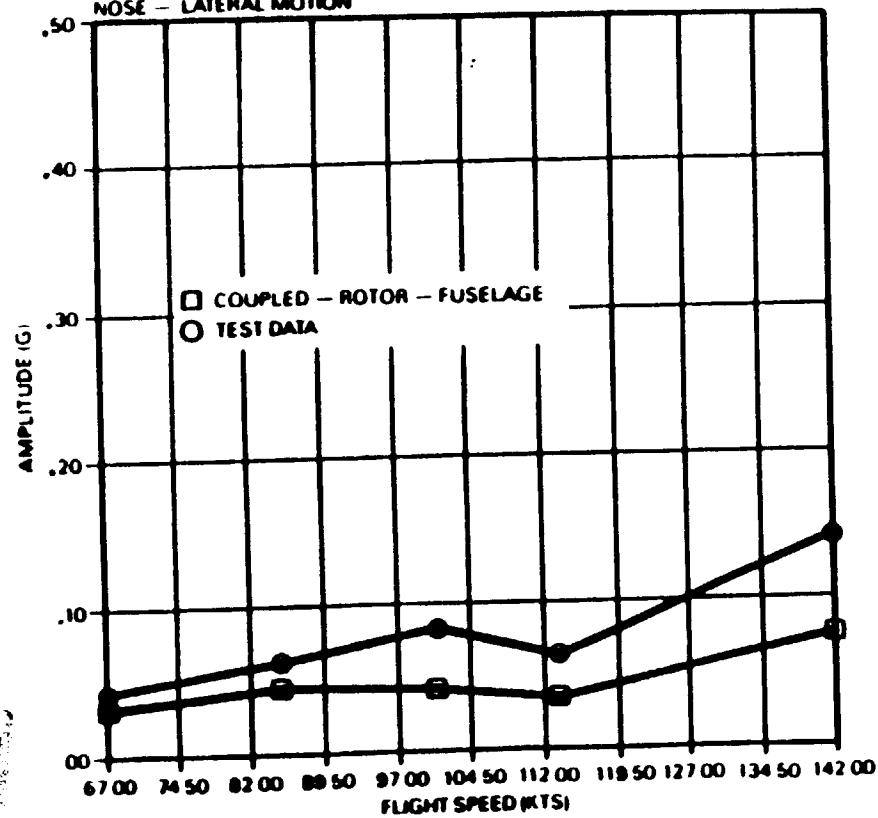
Nose 2P (Lateral and Vertical) Acceleration level against flight speed



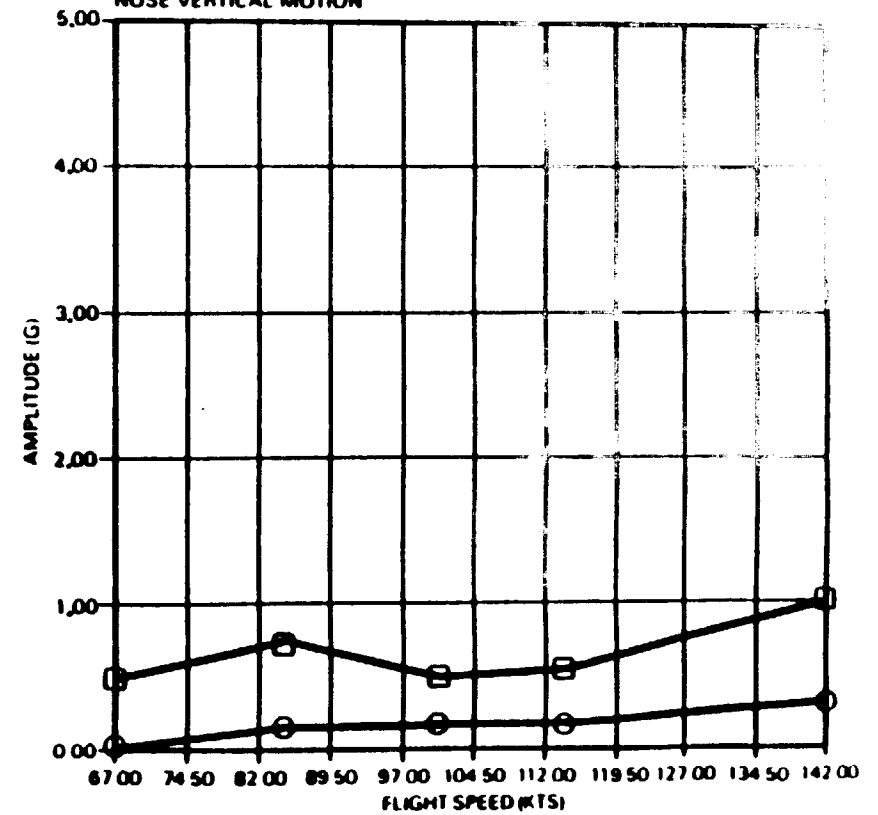
# RESULTS

Nose 2P (Lateral and Vertical) Acceleration level against flight speed

AH 1G 2P FUSELAGE VIBRATION LEVELS — FLIGHT 95A  
NOSE — LATERAL MOTION



AH 1G 2P FUSELAGE VIBRATION LEVELS — FLIGHT 95A  
NOSE VERTICAL MOTION



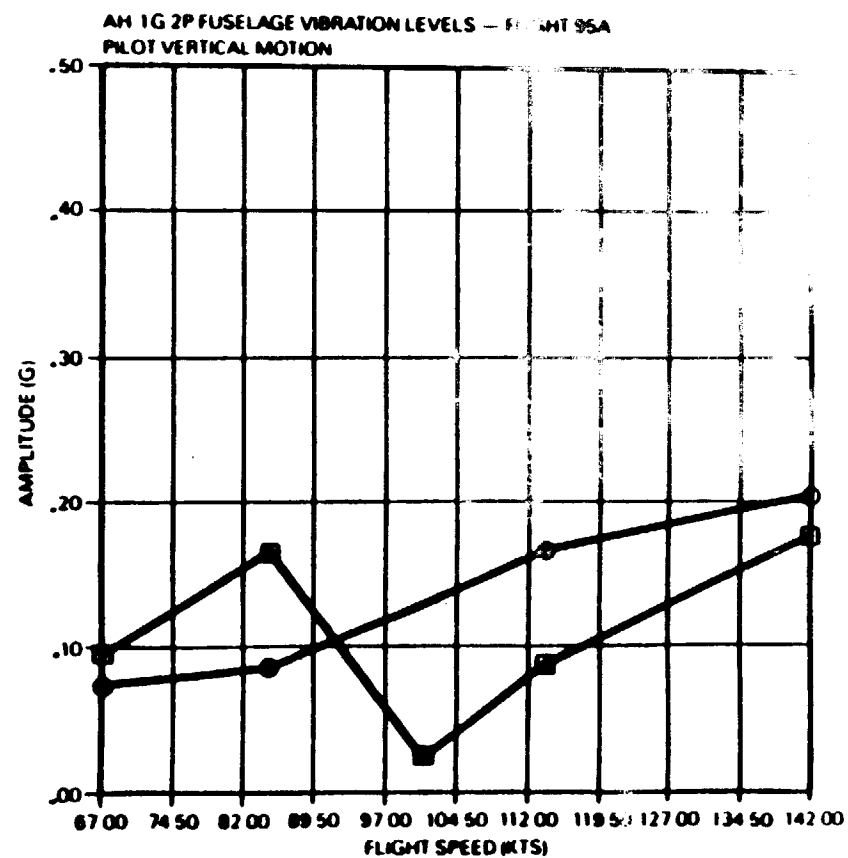
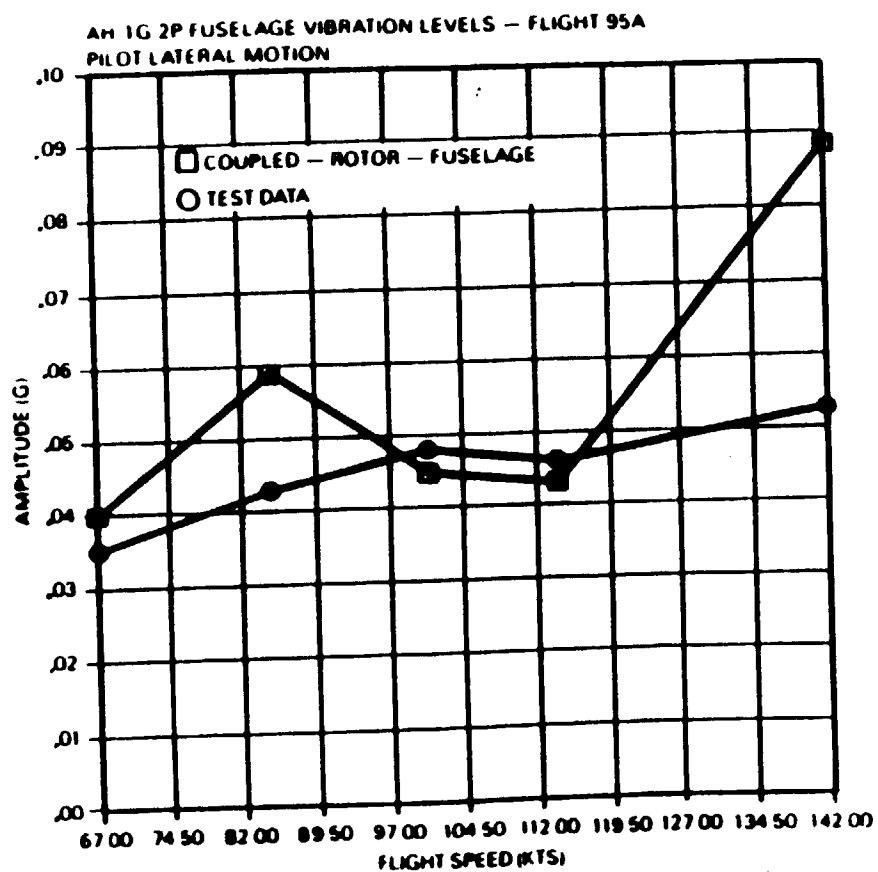
ORIGINAL PAGE IS  
OF POOR QUALITY

## **RESULTS**

**Pilot Seat 2P (Lateral and Vertical) Acceleration level against  
flight speed**

## RESULTS

Pilot Seat 2P (Lateral and Vertical) Acceleration level against flight speed



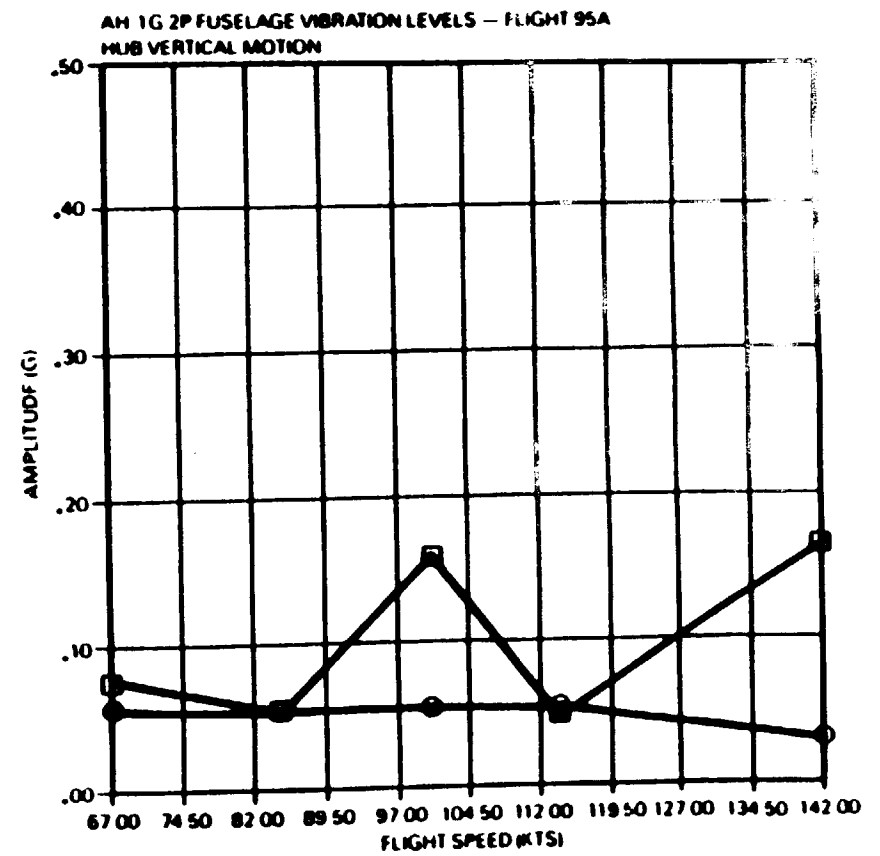
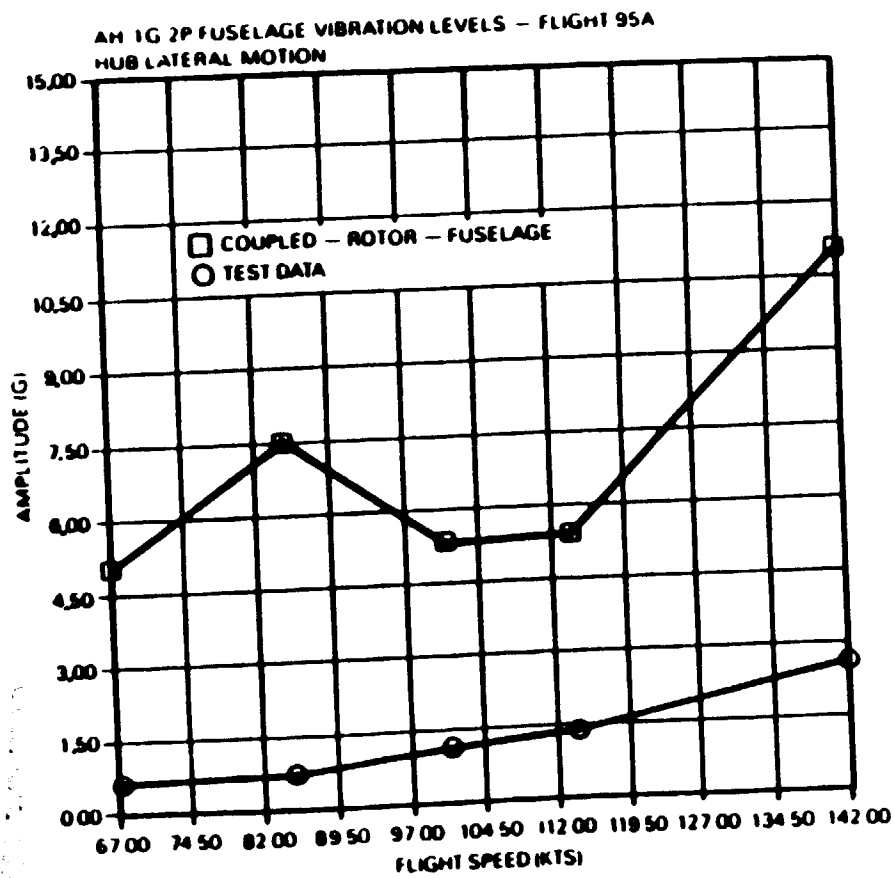
ORIGINAL PAGE IS  
OF POOR QUALITY

## RESULTS

Hub 2P (Lateral and Vertical) Acceleration level against  
flight speed

## RESULTS

Hub 2P (Lateral and Vertical) Acceleration level against flight speed

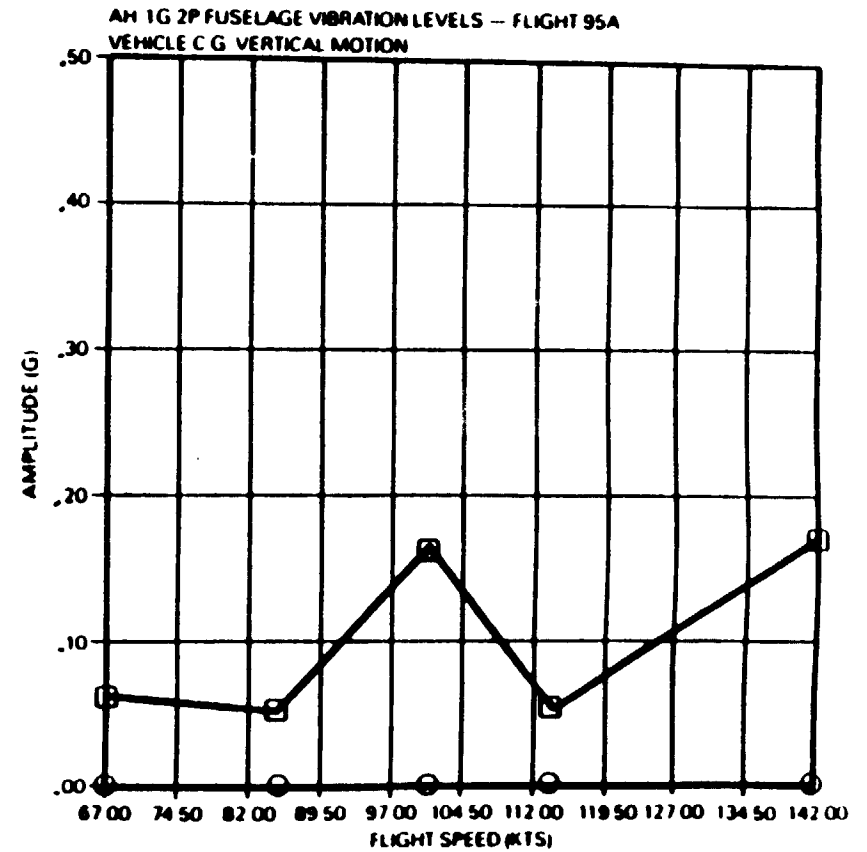
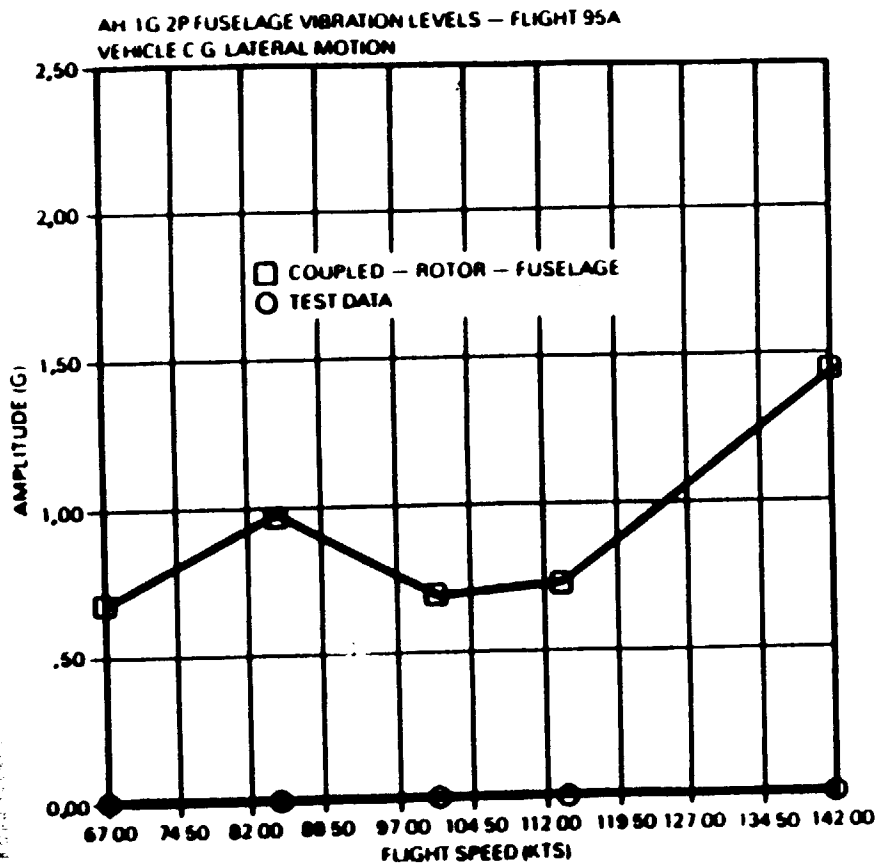


## **RESULTS**

**CG 2P (Lateral and Vertical) Acceleration level against  
flight speed**

## RESULTS

CG 2P (Lateral and Vertical) Acceleration level against flight speed



ORIGINAL PAGE IS  
OF POOR QUALITY

## **RESULTS**

**Gear box 2P (Lateral and Vertical) Acceleration level against  
flight speed**

**no lateral test data available**

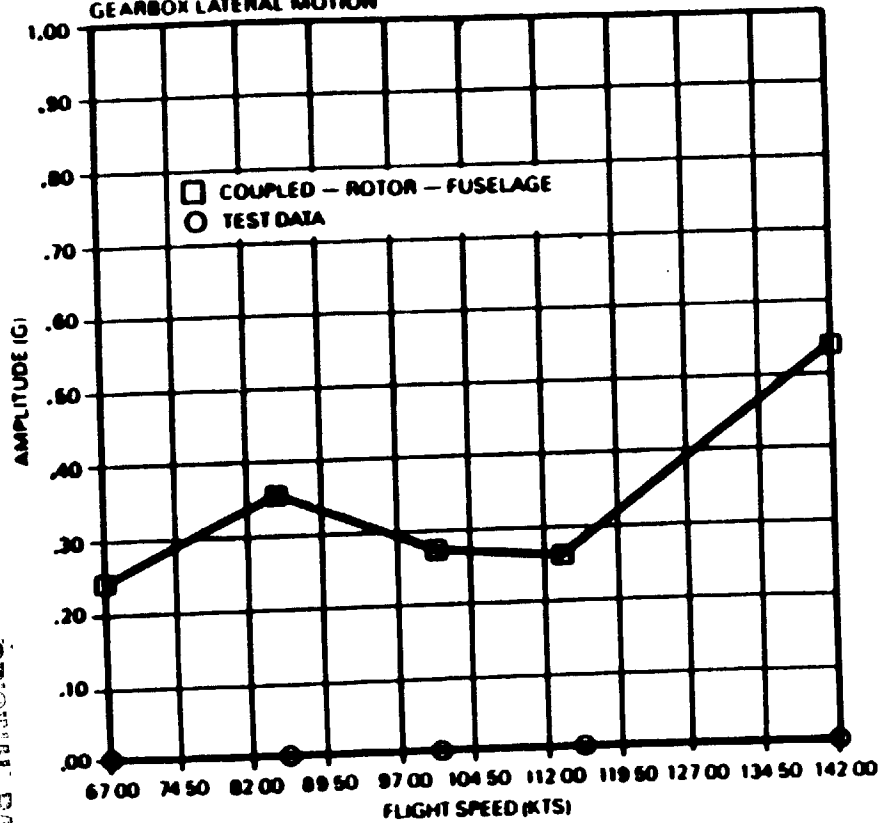


## RESULTS

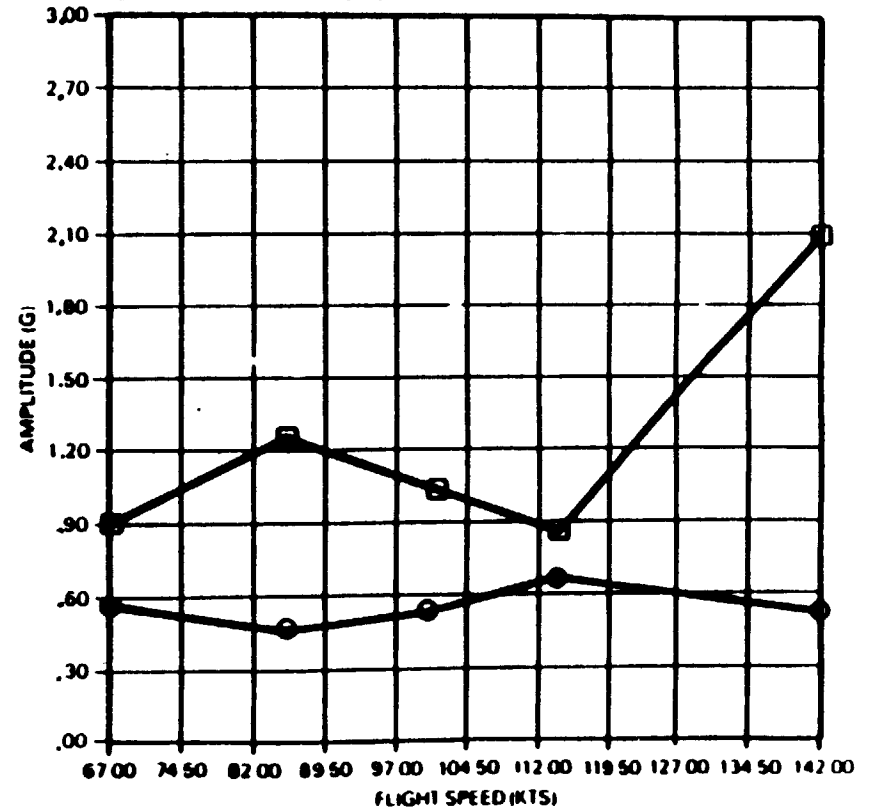
Gear box 2P (Lateral and Vertical) Acceleration level against flight speed

no lateral test data available

AH 1G 2P FUSELAGE VIBRATION LEVELS - FLIGHT 35A  
GEARBOX LATERAL MOTION



AH 1G 2P FUSELAGE VIBRATION LEVELS - FLIGHT 95A  
GEARBOX VERTICAL MOTION



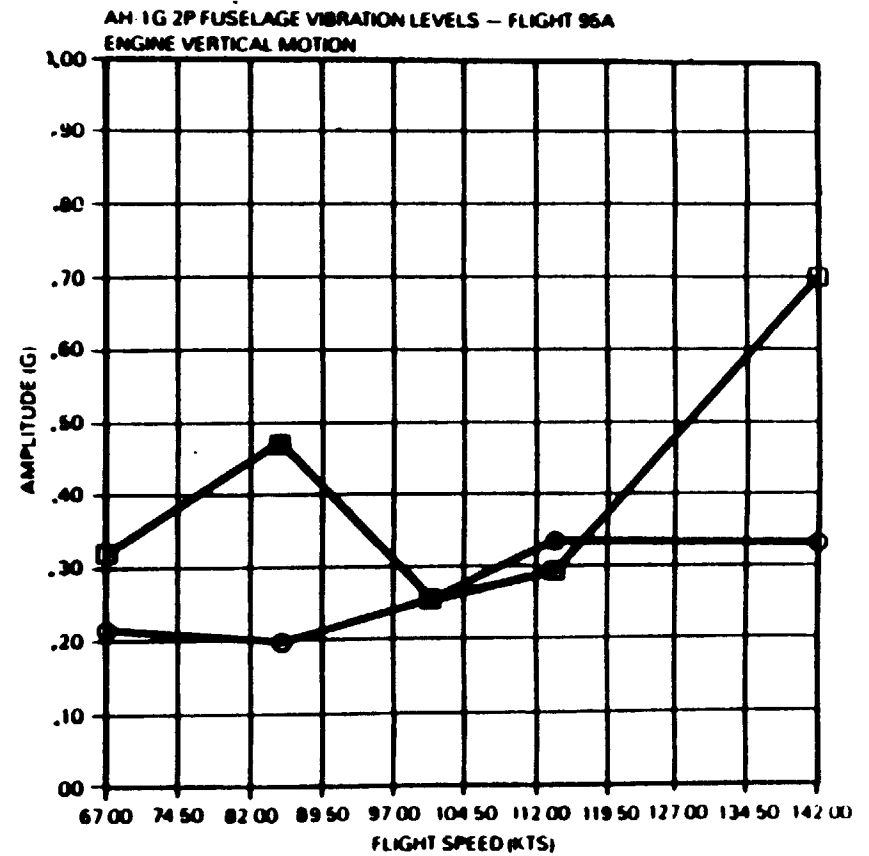
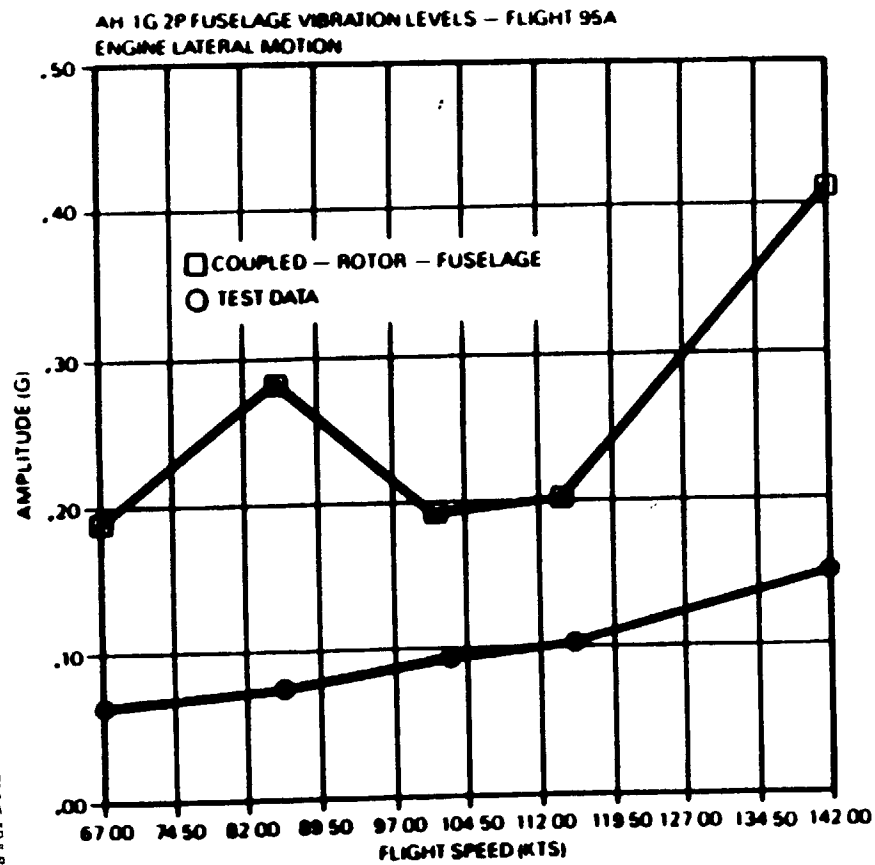
ORIGINAL PAGE IS  
OF POOR QUALITY

## **RESULTS**

**Engine 2P (Lateral and Vertical) Acceleration level against  
flight speed**

## RESULTS

Engine 2P (Lateral and Vertical) Acceleration level against  
flight speed



ORIGINAL PAGE IS  
OF GOOD QUALITY

## **RESULTS**

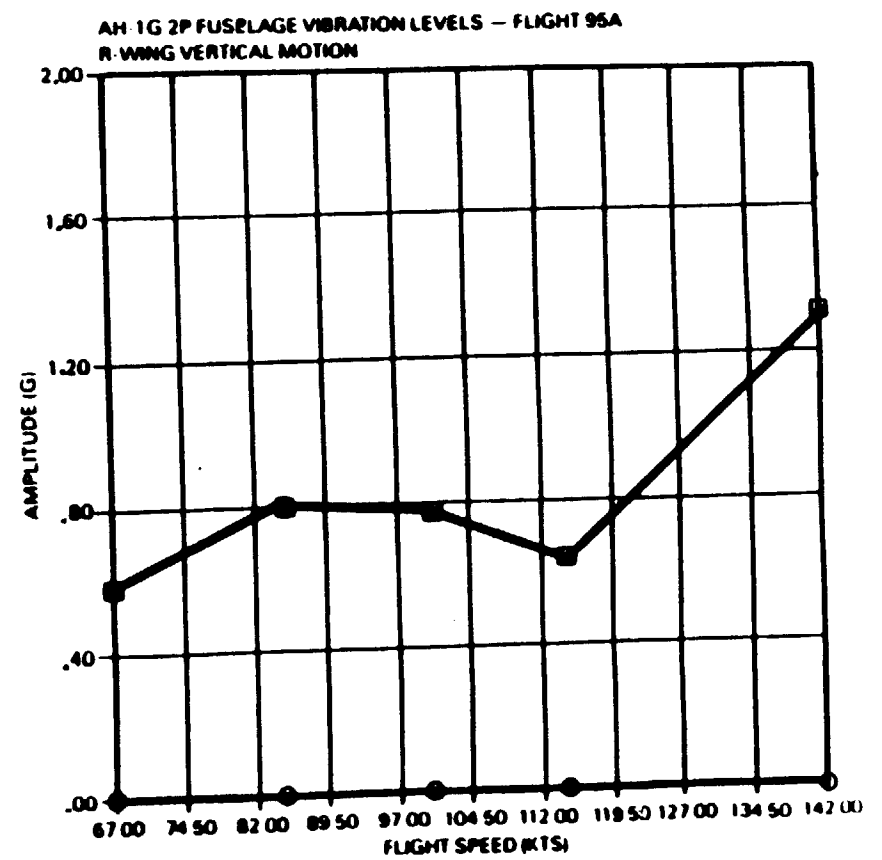
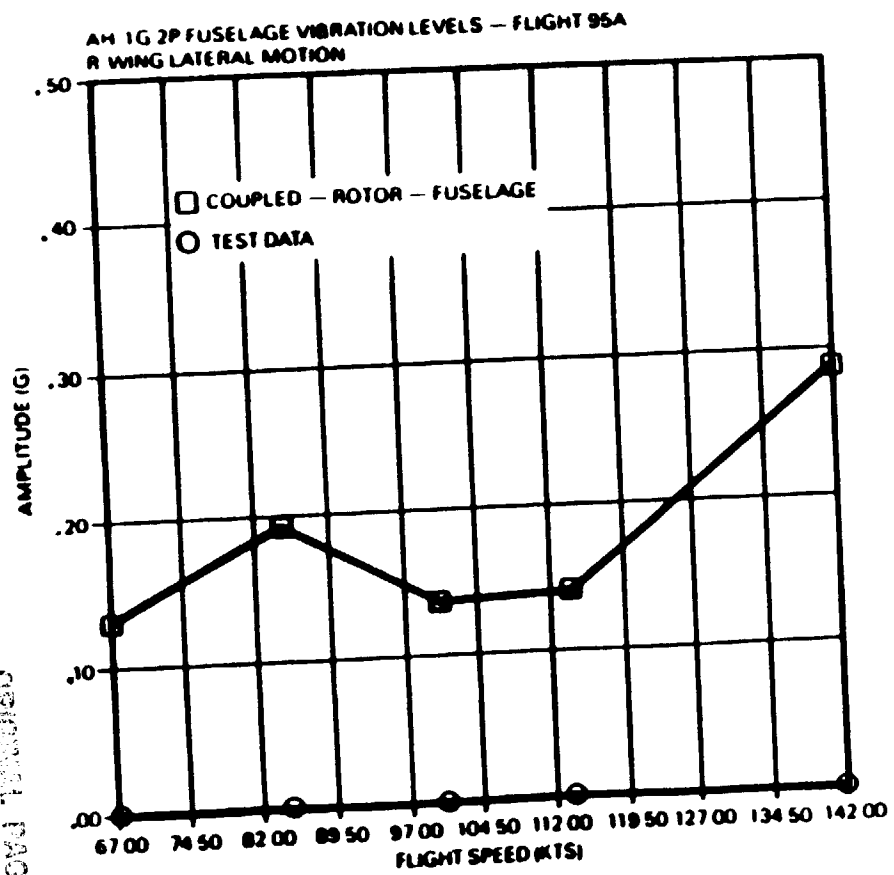
**R-Wing 2P (Lateral and Vertical) Acceleration level against  
flight speed**

**no test data available**

## RESULTS

R-Wing 2P (Lateral and Vertical) Acceleration level against flight speed

no test data available



ORIGINAL PAGE IS  
OF POOR QUALITY

## **RESULTS**

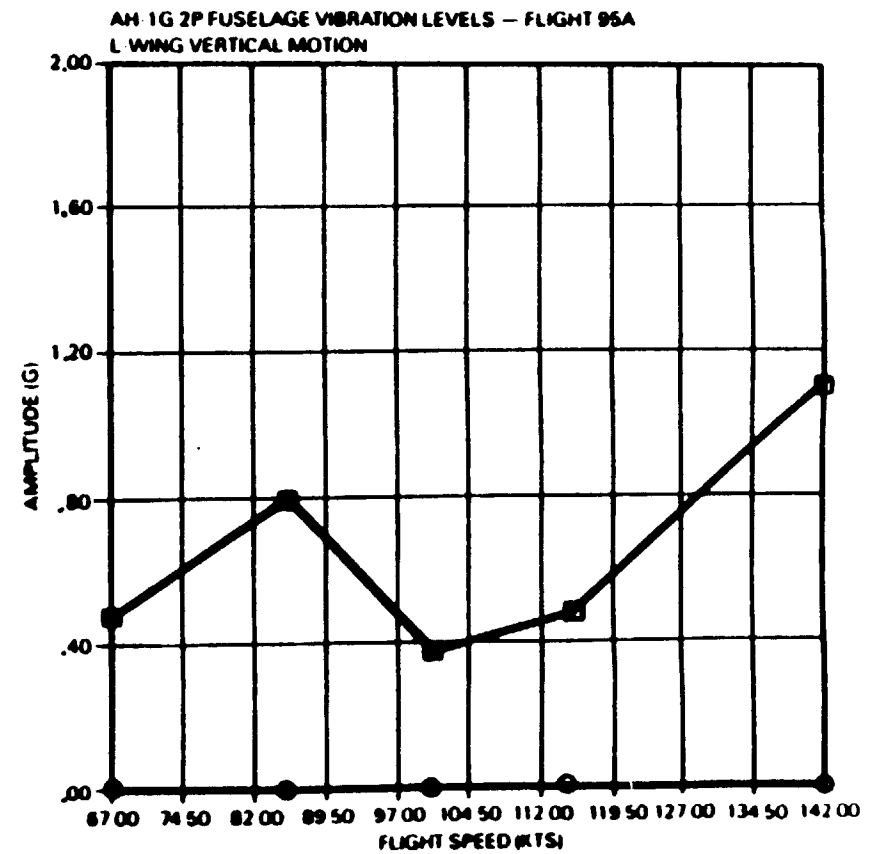
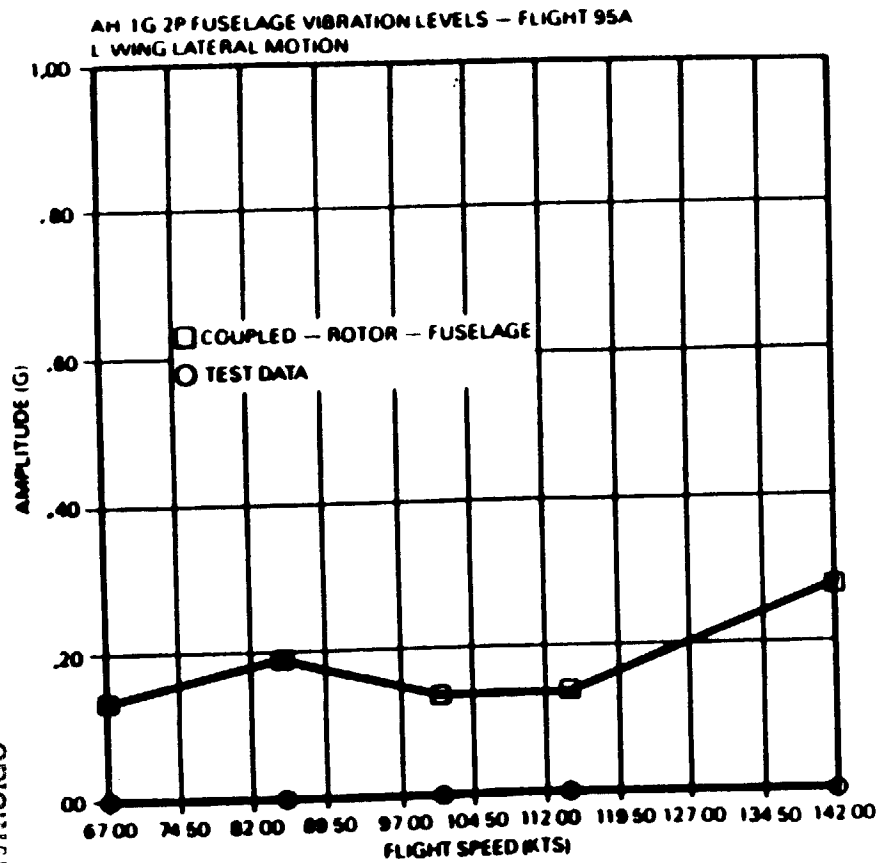
**L-Wing 2P (Lateral and Vertical) Acceleration level against  
flight speed**

**no test data available**

## RESULTS

L-Wing 2P (Lateral and Vertical) Acceleration level against  
flight speed

no test data available



ORIGINAL PAGE IS  
OF POOR QUALITY

## **RESULTS**

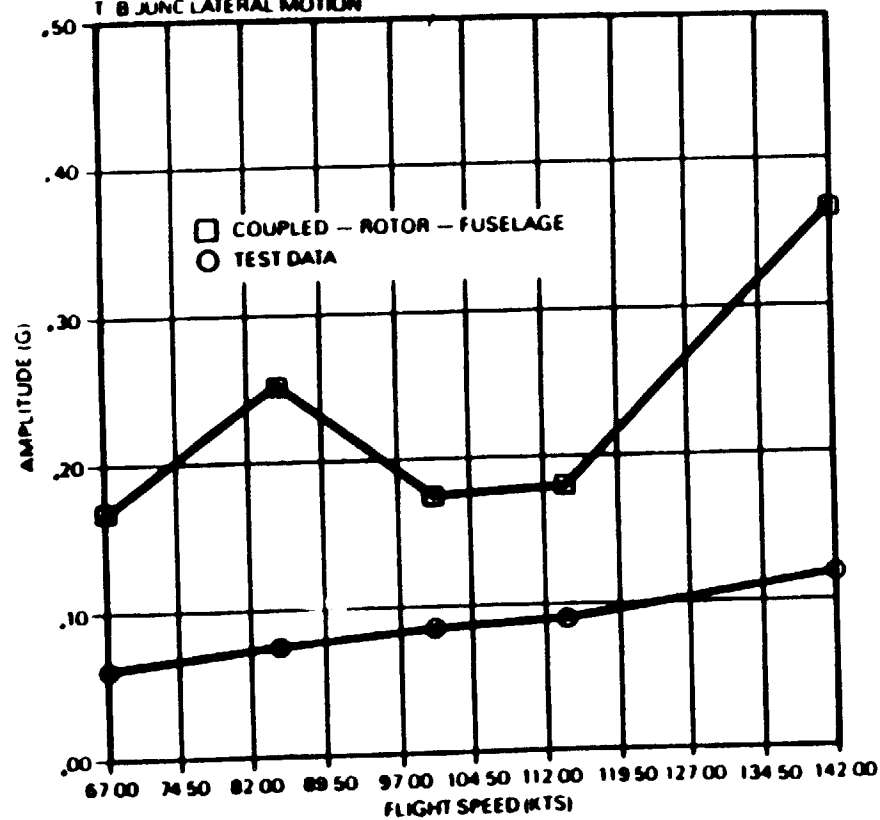
**T-B Junction 2P (Lateral and Vertical) Acceleration level against  
flight speed**



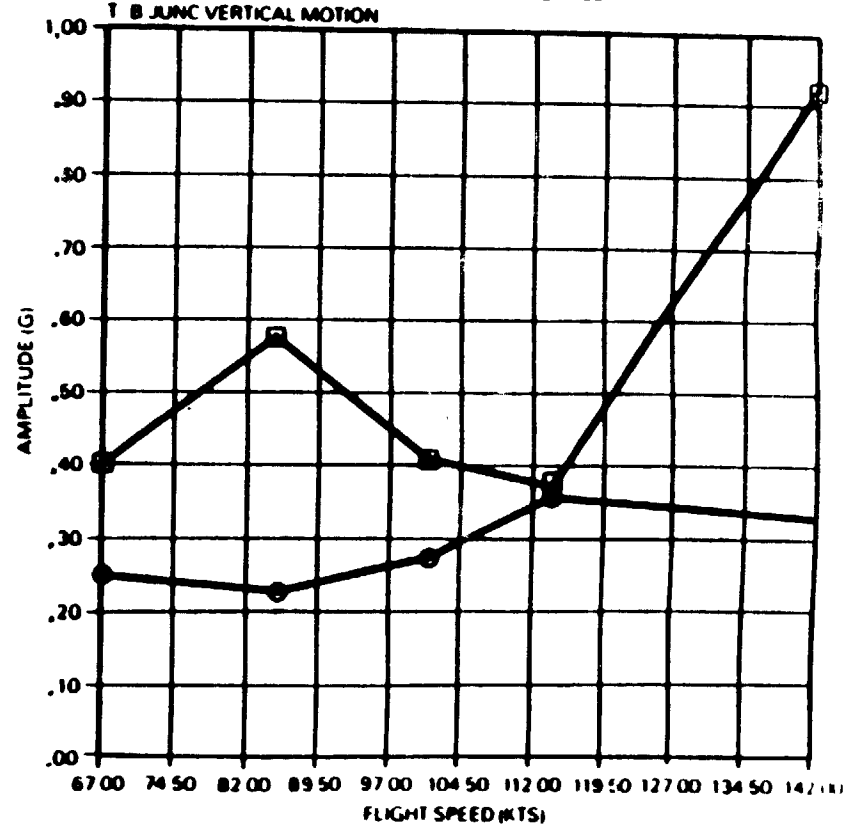
## RESULTS

T-B Junction 2P (Lateral and Vertical) Acceleration level against flight speed

AH 1G 2P FUSELAGE VIBRATION LEVELS - FLIGHT 95A  
T B JUNC LATERAL MOTION



AH 1G 2P FUSELAGE VIBRATION LEVELS - FLIGHT 95A  
T B JUNC VERTICAL MOTION



ORIGINAL PAGE IS  
OF POOR QUALITY

## **RESULTS**

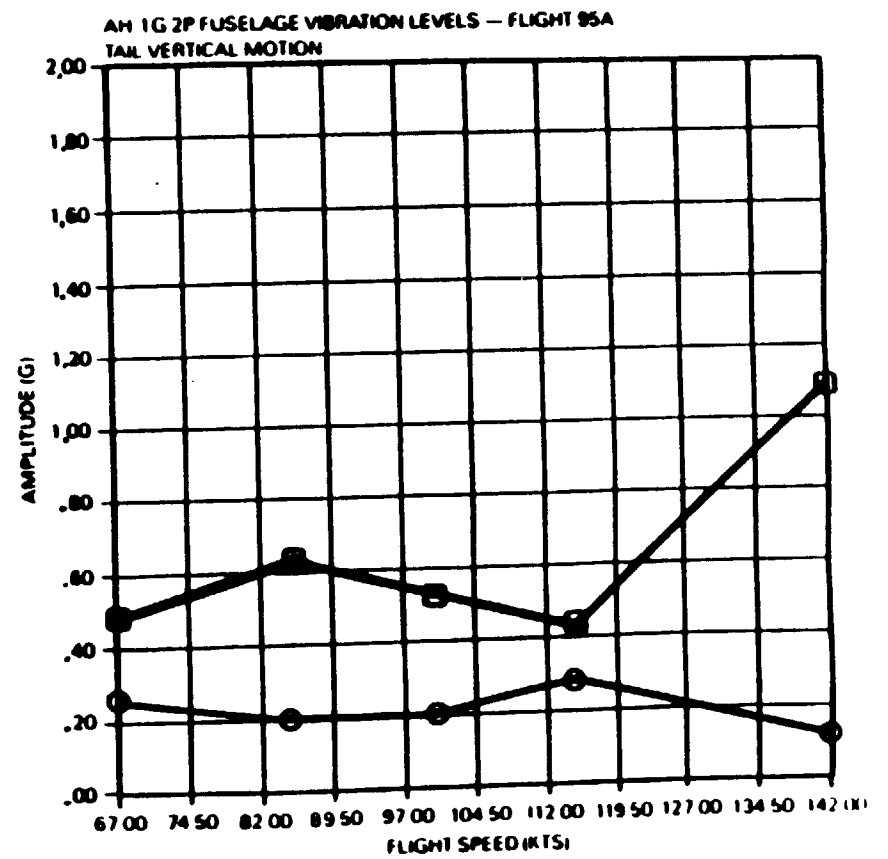
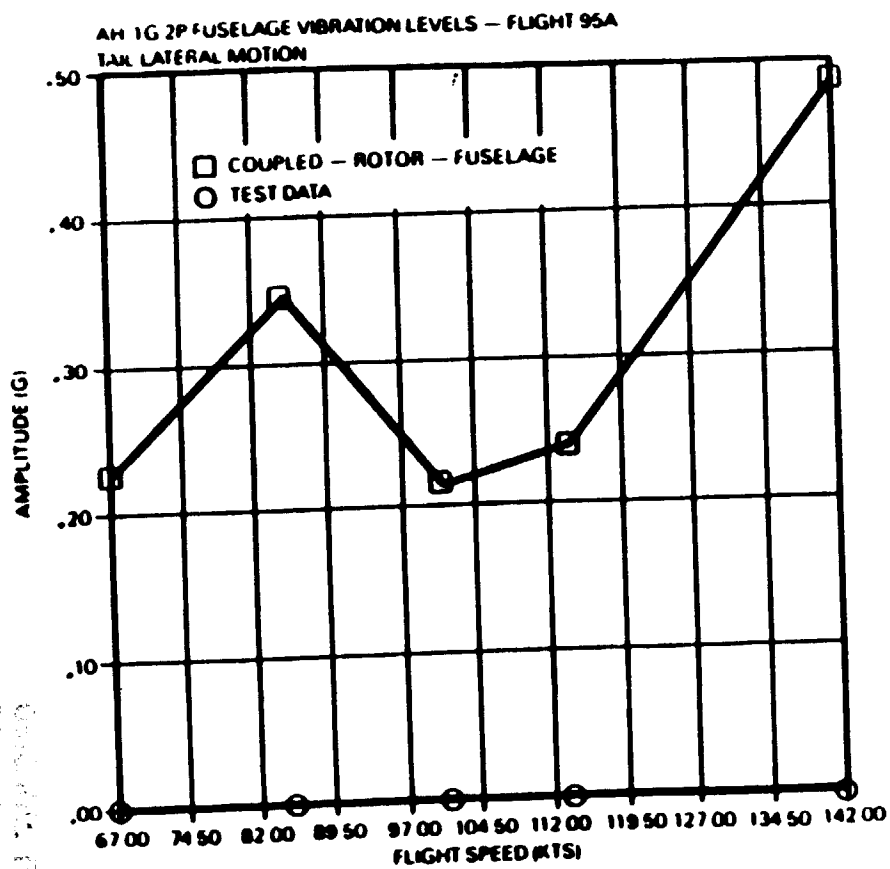
**Tail 2P (Lateral and Vertical) Acceleration level against  
flight speed**

**no lateral test data available**

## RESULTS

Tail 2P (Lateral and Vertical) Acceleration level against flight speed

no lateral test data available



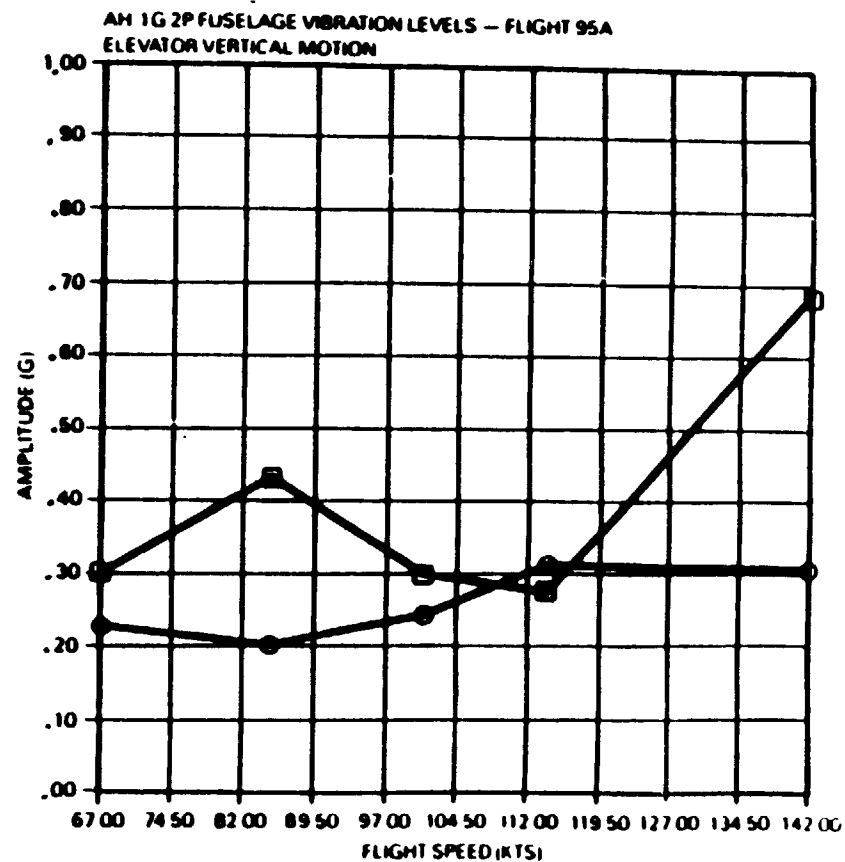
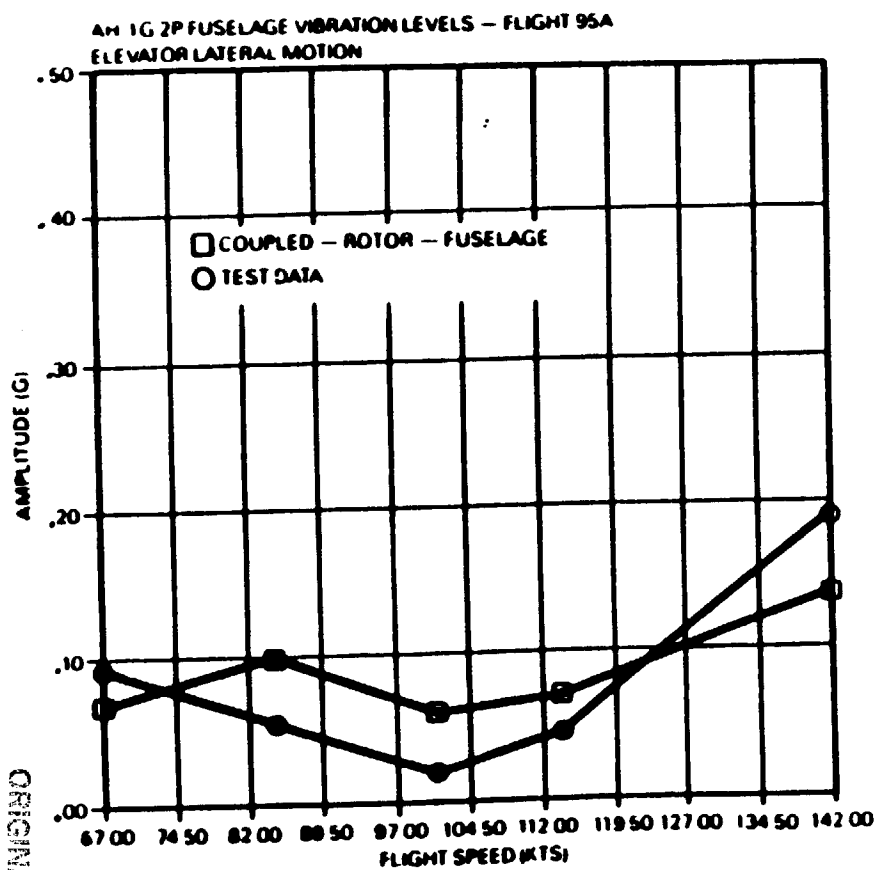
CONCERN: THERE IS  
OF POOR QUALITY

## **RESULTS**

**Elevator    2P (Lateral and Vertical) Acceleration level against  
                 flight speed**

## RESULTS

Elevator 2P (Lateral and Vertical) Acceleration level against flight speed



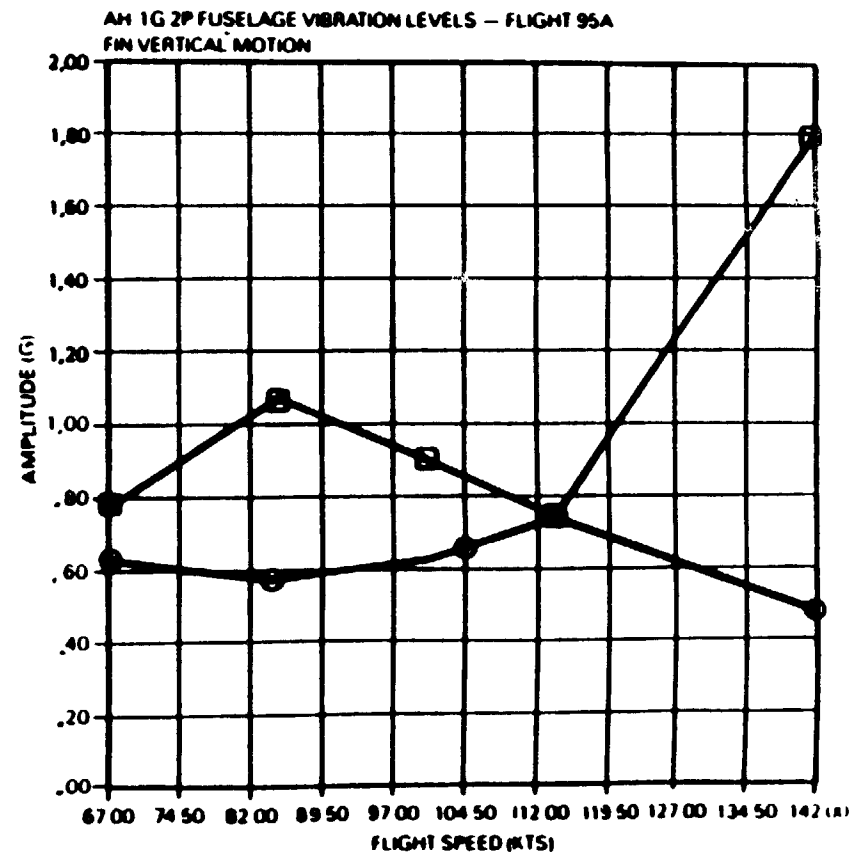
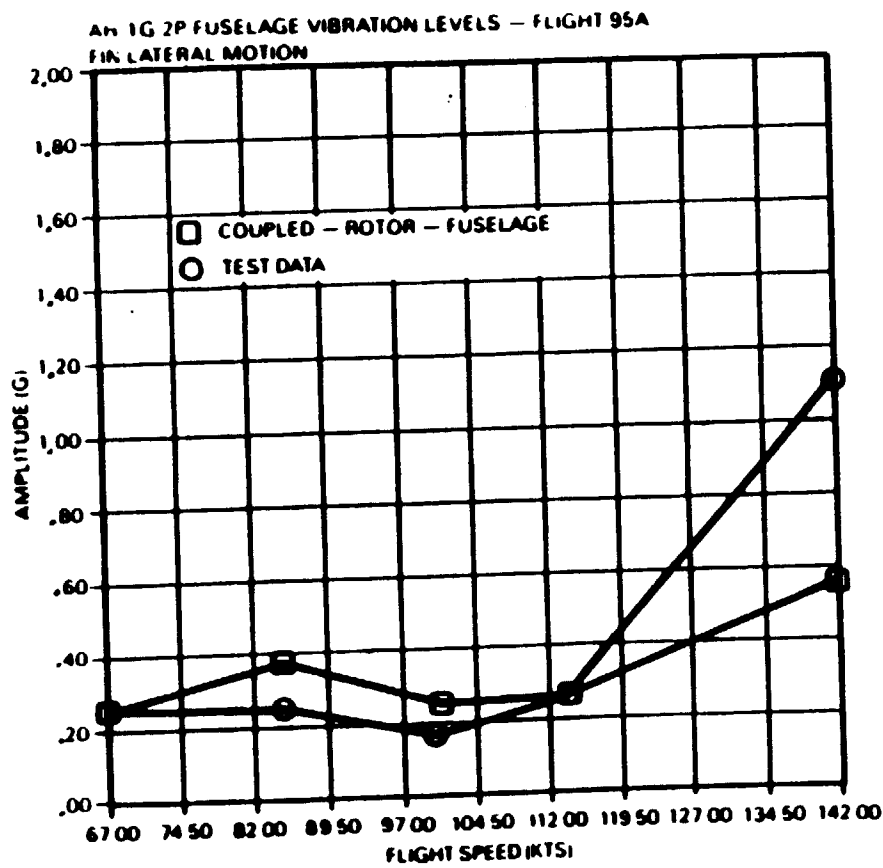
ORIGINAL PAGE IS  
OF POOR QUALITY

## **RESULTS**

**Fin 2P (Lateral and Vertical) Acceleration level against  
flight speed**

## RESULTS

Fin 2P (Lateral and Vertical) Acceleration level against flight speed



ORIGINAL PAGE IS  
OF POOR QUALITY





PRECEDING PAGE BLANK NOT FILMED

---

## 12.0 CONCLUDING REMARKS

## CONCLUDING REMARKS

A description and summary of MDHC's method for coupled rotor/airframe analysis, RACAP, has been presented in the above discussion. RACAP is capable of accurately modeling all rotor configurations, including teetering rotors, to determine rotor and fuselage forced response loads for a given flight condition. The analysis has been formulated to facilitate the use of different modules for inflow, rotor trim, unsteady aerodynamic airload calculations, and structural model root end boundary conditions. The modular approach allows the analyst to easily update the program and to investigate alternate analytical approaches to a particular part of the overall aeroelastic response problem.

A description of the results obtained using RACAP to model the AH-1G has also been presented. While the results indicate distinct trends, there are some questions regarding the input data. Free wake inflow generally indicated better correlation. Inclusion of wake-fuselage interaction in the aft regions may improve correlation.

In general, fairly good correlation is obtained for all flight conditions.

## **CONCLUDING REMARKS**

---

- **MDHC'S COUPLED ROTOR/AIRFRAME ANALYSIS, RACAP IS A COMPREHENSIVE AEROELASTIC PROGRAM THAT CAN ADEQUATELY MODEL ALL ROTOR CONFIGURATIONS**
- **RACAP HAS BEEN DEVELOPED WITH THE FLEXIBILITY TO INCORPORATE DIFFERENT STRUCTURAL AND AERODYNAMIC MODULES**
- **AH-1G MODELING SHOWS CONSISTENT AND FAIRLY ACCURATE FUSELAGE VIBRATION LEVEL CORRELATION**



PRECEDING PAGE BLANK NOT FILMED

---

## **13. REFERENCES**



## REFERENCES

1. Sadler, S. Gene: 'Development and Application of a Method for Predicting Rotor Free Wake Positions and Resulting Rotor Blade Airloads', NASA Contractor Report 1911, December 1971.

PRECEDING PAGE BLANK NOT FILMED





---

## APPENDIX 1

PREVIOUS EDITIONS IN ANK NOT FILMED



## APPENDIX 1

In order to evaluate the validity of the AH-1G Finite Element Model from a coupled rotor-fuselage vibration prediction standpoint, an analytical test was designed and performed. The test consisted of using the measured hub vibrations, and computing from these an estimate of the hub loads required to produce such vibrations. This relationship is

$$\begin{Bmatrix} F_X \\ F_Y \\ F_Z \end{Bmatrix} = [R_{HH}]^{-1} \begin{Bmatrix} \ddot{X} \\ \ddot{Y} \\ \ddot{Z} \end{Bmatrix} \quad (1)$$

In equation 1, the left hand side is an estimate of the hub loads required to produce the vibration level measured on the ship, the matrix  $R_{HH}$  is a matrix calculated from the fuselage finite element model, relating unit hub forces to hub vibrations, and the vector on the right hand side is the measured hub accelerations. By applying these hub forces to a transfer matrix relating hub forces to fuselage vibrations at any location of interest, L, one can compute the vibratory response at L. If the fuselage finite element model were exact, this vibration level at L would be equal to the measured quantity. This test was performed at all the locations at which test data was available, and did not provide good correlation at any of these locations. In particular, the lateral vibration levels are most in error, differing by up to 80 percent in magnitude. The vertical vibration magnitudes are significantly better, but still not adequate. These results lead to the conclusion that the fidelity of the NASTRAN model is less than adequate, or that there are additional factors affecting vibrations, not included in the model. The RACAP predicted hub loads and vibrations depend on the hub impedance as well as the fuselage transfer matrices, both of which are a function of the finite element model.

In conclusion, there are reasons to suspect the validity of the NASTRAN model, and these provide some of the reasons for errors in the predicted fuselage vibratory response.

PRECEDING PAGE BLANK NOT FILMED



## Report Documentation Page

1. Report No. NASA CR-181974		2. Government Accession No.		3. Recipient's Catalog No.	
4. Title and Subtitle CORRELATION OF AH-1G AIRFRAME FLIGHT VIBRATION DATA WITH A COUPLED ROTOR-FUSELAGE ANALYSIS				5. Report Date AUGUST 1990	
				6. Performing Organization Code	
7. Author(s) K. SANGHA AND J. SHAMIE				8. Performing Organization Report No.	
				10. Work Unit No. 505-63-51-01	
9. Performing Organization Name and Address MCDONNELL DOUGLAS HELICOPTER COMPANY 5000 E. MCDOWELL ROAD MESA, ARIZONA 85205-9797				11. Contract or Grant No. NAS1-17498	
				13. Type of Report and Period Covered CONTRACTOR REPORT	
12. Sponsoring Agency Name and Address NASA LANGLEY RESEARCH CENTER HAMPTON, VIRGINIA 23665-5225				14. Sponsoring Agency Code	
15. Supplementary Notes LANGLEY TECHNICAL MONITOR: DR. RAYMOND G. KVATERNIK					
16. Abstract The formulation and features of the McDonnell Douglas Helicopter Company (MDHC) Rotor-Airframe Comprehensive Analysis Program (RACAP) is described. The analysis employs a frequency domain, transfer matrix approach for the blade structural model, a time domain wake or momentum theory aerodynamic model and impedance matching for rotor-fuselage coupling. The analysis is applied to the AH-1G helicopter, and a correlation study is conducted on fuselage vibration predictions. The purpose of the study is to evaluate the state-of-the-art in helicopter fuselage vibration prediction technology. The fuselage vibrations predicted using RACAP are fairly good in the vertical direction and somewhat deficient in the lateral/longitudinal directions. Some of these deficiencies are traced to the fuselage finite-element model.					
17. Key Words (Suggested by Author(s)) TRANSFER MATRIX APPROACH, COUPLED ROTOR-FUSELAGE, HARMONIC BALANCE, IMPEDANCE MATCHING, VIBRATION, RACAP, NASTRAN			18. Distribution Statement UNCLASSIFIED -- UNLIMITED  Subject Category 39		
19. Security Classif. (of this report) UNCLASSIFIED		20. Security Classif. (of this page) UNCLASSIFIED		21. No. of pages 228	
				22. Price A11	